

Rational Design of Dipicolylamine-Containing Carbazole Amphiphiles Combined with Zn²⁺ as Potent Broad-Spectrum Antibacterial Agents with a Membrane-Disruptive Mechanism

Jiayong Liu,[#] Hongxia Li,[#] Haizhou Li, Shanfang Fang, Jinguo Shi, Yongzhi Chen, Rongcui Zhong, Shouping Liu,^{*} and Shuimu Lin^{*}



Cite This: *J. Med. Chem.* 2021, 64, 10429–10444



Read Online

ACCESS |



Metrics & More

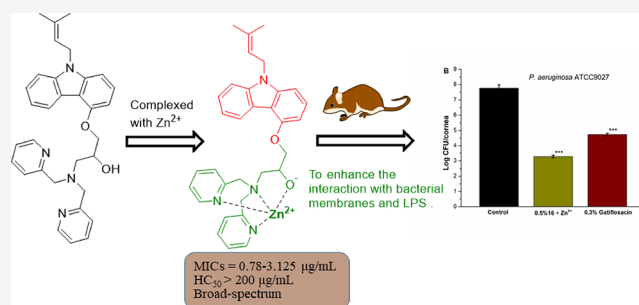


Article Recommendations



Supporting Information

ABSTRACT: Antibiotic resistance has become one of the most urgently important problems facing healthcare providers. A novel series of dipicolylamine-containing carbazole amphiphiles with strong Zn²⁺ chelating ability were synthesized, biomimicking cationic antimicrobial peptides. Effective broad-spectrum **16** combined with 12.5 μg/mL Zn²⁺ was identified as the most promising antimicrobial candidate. **16** combined with 12.5 μg/mL Zn²⁺ exhibited excellent antimicrobial activity against both Gram-positive and Gram-negative bacteria (MICs = 0.78–3.125 μg/mL), weak hemolytic activity, and low cytotoxicity. Time-kill kinetics and mechanism studies revealed **16** combined with 12.5 μg/mL Zn²⁺ had rapid bacterial killing properties, as evidenced by disruption of the integrity of bacterial cell membranes, effectively preventing bacterial resistance development. Importantly, **16** combined with 12.5 μg/mL Zn²⁺ showed excellent *in vivo* efficacy in a murine keratitis model caused by *Staphylococcus aureus* ATCC29213 or *Pseudomonas aeruginosa* ATCC9027. Therefore, **16** combined with 12.5 μg/mL Zn²⁺ could be a promising candidate for treating bacterial infections.



INTRODUCTION

Antibiotic resistance has become a global health challenge and poses a serious threat to human health.^{1–3} It is reported that approximately 700,000 deaths worldwide are caused by drug-resistant bacterial infections each year, including more than 23,000 deaths in the United States and 175,000 deaths in the European Union.^{4–6} Since the 1980s, the discovery and development of new antibacterial agents have been very slow, and the number of newly approved antibacterial agents has been severely reduced.^{7,8} In addition, no new drugs have been approved for treating Gram-negative bacterial infections in the past three decades.^{7,8} Gram-negative bacteria have special outer membranes that consist of a lipopolysaccharide (LPS) layer and membrane phospholipids, making it very difficult for most antibiotics to penetrate the cell membranes to show effective antibacterial efficacy.^{9,10} In a global priority list of antibiotic-resistant bacteria published by the World Health Organization in 2017, the listed bacteria of critical priority are all Gram-negative bacteria, including carbapenem-resistant *Acinetobacter baumannii* and *Pseudomonas aeruginosa*, as well as extended-spectrum β-lactamase (ESBL)-producing carbapenem-resistant *Enterobacteriaceae*.¹¹ Therefore, in the current serious situation, it is urgent to develop new broad-spectrum antibacterial agents that can overcome drug-resistant bacterial infections.¹²

Cationic antimicrobial peptides (CAMPs) are widely distributed in various organisms as immune response products and possess a variety of biological activities.^{13–15} The cationic amphiphilic conformation of CAMPs plays a vital role in their antimicrobial effects.^{16,17} The cationic region of CAMPs is attracted by negatively charged bacterial cell membranes via electrostatic interactions, and then the lipophilic/hydrophobic region of CAMPs is inserted into the lipid bilayer of the bacterial cell membranes to penetrate or destroy the membrane, leading to the leakage of intracellular contents and bacterial death.^{14,18–20} This membrane-targeting mode of action is very helpful in greatly reducing the probability of bacterial resistance.^{14,21,22} However, poor *in vivo* stability and efficacy, poor pharmacokinetic properties, high cytotoxicity, and expensive preparation costs are common and notable obstacles for the use of CAMPs as antimicrobials in clinical applications.²³ Recently, research on small molecule mimetics of CAMPs has provided a very promising solution to overcome

Received: May 12, 2021

Published: July 8, 2021



these problems associated with CAMPs.^{24,25} Our group and other laboratories previously discovered and optimized flavone,^{26,27} xanthone,^{28,29} and aminoglycoside^{30,31}-based peptidomimetics by biomimicking the structure and function of CAMPs. Several successful examples, such as LTX-109 and brilacidin, have entered or finished phase 2 clinical trials.^{32,33}

Carbazole derivatives have many pharmacological activities,^{34–37} including anti-inflammatory,³⁸ antibacterial,³⁹ antifungal,⁴⁰ antitumor,⁴¹ antioxidant activities,⁴² etc. The commercial antihypertensive drugs carazolol and carvedilol possess carbazole scaffolds.^{36,37} In our previous work, we used 4-epoxypropoxycarbazole as the starting material to design and synthesize a series of carbazole-based antimicrobial agents by biomimicking CAMPs.⁴³ The lead compound (Figure 1)

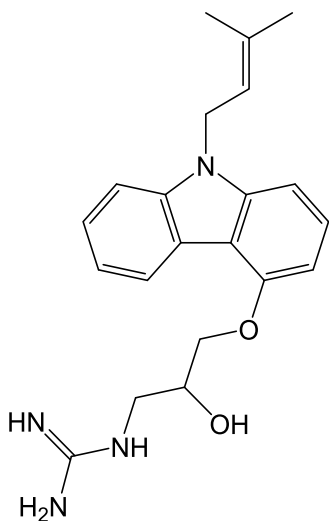


Figure 1. Chemical structure of the carbazole-based lead compound.

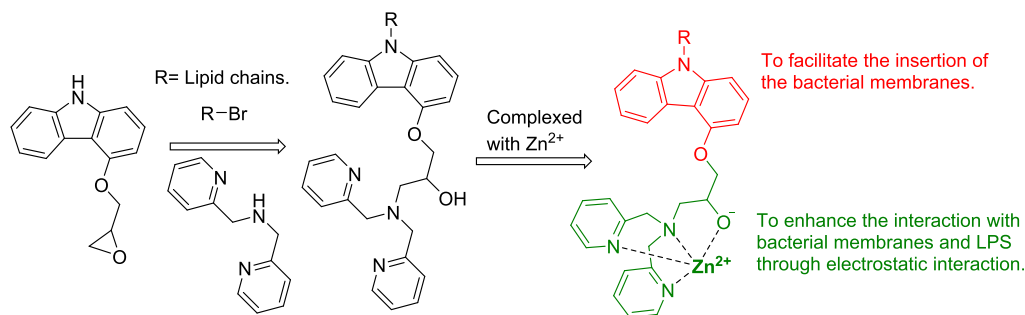
containing guanidine and isoprenyl groups exhibited excellent *in vitro* and *in vivo* anti-Gram-positive bacterial activity, killed bacteria rapidly by destroying the bacterial membranes, and effectively avoided the development of bacterial resistance.⁴³ However, these cationic carbazole-based compounds displayed poor antibacterial activity against Gram-negative bacteria.⁴³ The main reason may be that these synthesized carbazoles had poor penetration/diffusion ability through the outer membrane barrier (LPS layer) of Gram-negative bacteria, making it very difficult for them to enter the cell membranes of Gram-negative bacteria to exert antibacterial activity.⁴³

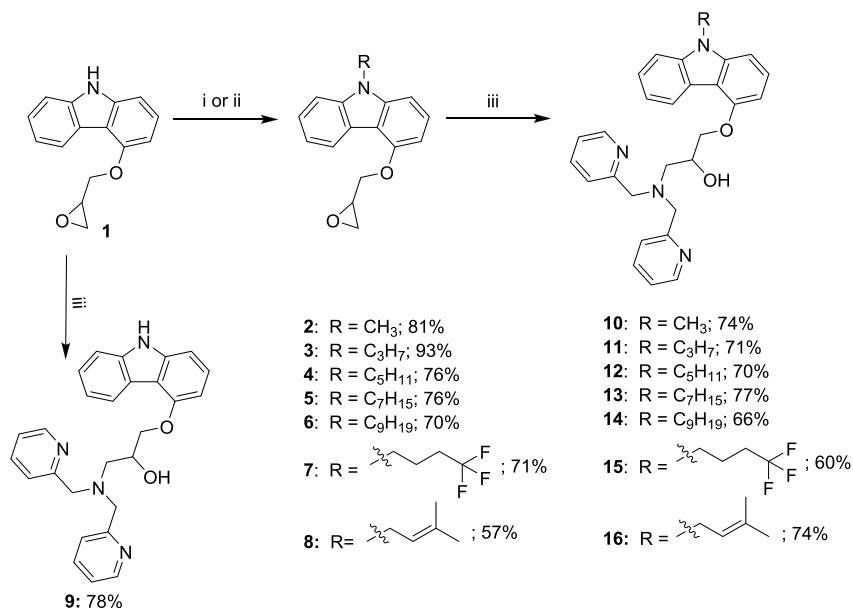
Metal ion complexes in biological systems have been widely studied due to their unique structures and properties.⁴⁴ Several

antibacterial compounds, including daptomycin^{45–47} and quinolones^{48,49} can form metal ion complexes by interacting with metal ions (e.g., Ca^{2+} , Zn^{2+} , and Mg^{2+}) to significantly enhance their antibacterial activity. Metal ions that act as electron acceptors show stronger electron-accepting abilities than H^+ .⁵⁰ The surface of bacterial cell membranes contains anionic phospholipids, such as phosphatidylglycerol (PG) and cardiolipin (CL).⁵¹ After the ligand and metal ions form complexes, the positive charge density of the ligand is enhanced.^{44,50} The formed complexes can strongly bind to anionic phospholipids on bacterial cell membranes.^{44,52} Zn^{2+} works as an essential trace element in the human body and participates in different types of life activities.⁵³ It is estimated that the total concentration of Zn^{2+} in mammalian cells is approximately 6.54–32.69 $\mu\text{g/mL}$.^{54,55} It has been reported that Zn^{2+} can specifically combine with dipicolylamine to form a Zn^{2+} -dipicolylamine (Zn -DPA) complex that binds to pyrophosphate with high affinity.^{52,56} In a positively charged metal complex, Zn^{2+} can effectively interact with negatively charged membranes of both Gram-positive and Gram-negative bacterial cells.^{43,57,58} As a selective membrane-targeting agent, the Zn -DPA complex has been widely used in cancer detection,⁵⁹ the treatment of neurodegenerative diseases,⁶⁰ and bacterial infections.^{43,57,58}

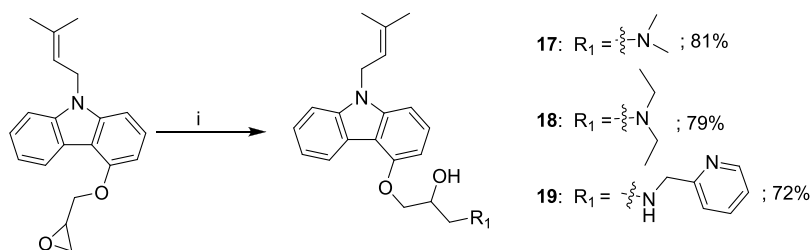
Inspired by the amphiphilic structure and function of CAMPs as well as the high affinity between the Zn -DPA complex and pyrophosphate, we designed a new series of amphiphilic dipicolylamine-containing carbazole derivatives combined with Zn^{2+} as antibacterial agents. In this study, we used 4-epoxypropoxycarbazole as the starting material, which is a commercially available intermediate for the preparation of carvedilol and carazolol,^{36,37} and different hydrophobic lipid chains were introduced into the carbazole scaffold to adjust the hydrophobicity of the carbazole compounds (Scheme 1). The cationic group of 2,2'-dipicolylamine with a strong chelating ability for Zn^{2+} was incorporated into the carbazole scaffold to yield a series of cationic carbazole amphiphiles. Based on the structural properties and hypothesis mentioned above, the designed compounds combined with Zn^{2+} were expected to overcome the limitation of permeation/diffusion through the outer membrane barrier (LPS layer) of Gram-negative bacteria. In the presence of Zn^{2+} , the designed dipicolylamine-containing carbazole compounds display significantly enhanced antibacterial activity against both Gram-positive and Gram-negative bacteria. After a series of structural optimization and biological activity evaluations, compound 16 combined with Zn^{2+} was identified as the most promising antimicrobial candidate that displayed excellent broad-spectrum antibacterial

Scheme 1. Design Concept for Amphiphilic Dipicolylamine-Containing Carbazole Derivatives Combined with Zn^{2+} as Antibacterial Agents by Biomimicking CAMPs



Scheme 2. Synthesis of Carbazole-Based Compounds 2–16^a

^aReagents and conditions: (i) 1-iodoalkanes, NaOH, DMF, 60 °C, 2 h. (ii) 3, 3-dimethylallyl bromide, KI, potassium *tert*-butoxide, DMF, 50 °C, 0.5 h. (iii) 2,2'-dipicolylamine, MeOH, reflux, 6 h.

Scheme 3. Synthesis of Carbazole-Based Compounds 17–19^a

^aReagents and conditions: (i) corresponding amines, MeOH, reflux, 6 h.

activity and weak hemolytic activity. The time-killing curve, development of drug resistance, mode of action, *in vitro* cytotoxicity toward mammalian cells, and *in vivo* efficacy in a murine bacterial keratitis model were further studied. This new design strategy provides a new solution for the discovery and development of effective broad-spectrum antibacterial agents to combat bacterial resistance.

RESULTS AND DISCUSSIONS

Design and Synthesis of Carbazole-Based Derivatives. In this study, we further designed and modified cationic amphiphilic carbazole derivatives for screening and identification of broad-spectrum antimicrobial compounds to overcome bacterial resistance. The chemical structures and synthetic routes of a new series of dipicolylamine-containing carbazole derivatives are shown in Schemes 2 and 3. Starting material **1** (4-epoxypropanoxycarbazole) was reacted with 3,3-dimethylallyl bromide or 1-iodoalkane in the presence of K₂CO₃ to yield intermediate compounds **2–8**. Then, compounds **1–8** were treated with 2,2'-dipicolylamine in methanol to give compounds **9–16**. Compounds **17–19** were prepared by the treatment of compound **8** with the corresponding amines. All synthesized compounds were characterized by H NMR, C NMR, and HRMS. The formation of compound **16-Zn²⁺** complexes was validated by mass

spectrometry, as indicated by the peak at *m/z* 569.3 (Figure S1, Supporting Information).

In Vitro Antibacterial and Hemolytic Activity. The minimum inhibitory concentrations (MICs) were used to evaluate the *in vitro* antibacterial activity of these synthetic carbazole derivatives in the presence of different concentrations of Zn²⁺ (0, 6.25, and 12.5 μg/mL) against a panel of Gram-positive and Gram-negative bacteria, including *S. aureus* ATCC29213, MRSA NCTC10442, MRSA N315, *E. coli* ATCC25922, *P. aeruginosa* ATCC9027, *Acinetobacter baumannii* ATCC17978, and *A. baumannii* R2889 (Tables 1 and 2 and Table S1). Commercially available vancomycin and ciprofloxacin were used as positive controls. The hemolytic activity was evaluated by HC₅₀ values that were measured as the concentration required to lyse 50% of rabbit red blood cells.

Evaluation of the Influence of Zn²⁺ on the Activity. Zn²⁺, as a strong electron-acceptor, could greatly enhance the electron absorption property of cationic moieties of carbazole derivatives after being chelated to dipicolylamine groups, leading to a significant increase in their interaction with LPS or lipoteichoic acid (LTA), as well as negatively charged bacterial cell membranes. As shown in Table 2 and Table S1, compounds **9–16** with a cationic group of dipicolylamine combined with Zn²⁺ (6.25 or 12.5 μg/mL) showed a significant enhancement in antibacterial activity against

Table 1. Antibacterial and Hemolytic Activities of 12.5 $\mu\text{g/mL}$ Zn^{2+} and Compounds 1–19

compd	MIC ($\mu\text{g/mL}$)							HC_{50} ($\mu\text{g/mL}$)
	<i>S. aureus</i> ATCC 29213	MRSA N315	MRSA NCTC10442	<i>E. coli</i> ATCC25922	<i>P. aeruginosa</i> ATCC9027	<i>A. baumannii</i> ATCC17978	<i>A. baumannii</i> R2889	
Zn^{2+}	>50	>50	>50	>50	>50	>50	>50	>200
1	>50	>50	>50	>50	>50	>50	>50	>200
2	>50	>50	>50	>50	>50	>50	>50	>200
3	>50	>50	>50	>50	>50	>50	>50	>200
4	>50	>50	>50	>50	>50	>50	>50	>200
5	>50	>50	>50	>50	>50	>50	>50	>200
6	>50	>50	>50	>50	>50	>50	>50	>200
7	>50	>50	>50	>50	>50	>50	>50	ND ^a
8	>50	>50	>50	>50	>50	>50	>50	>200
9	25	25	25	>50	>50	50	>50	>200
10	12.5	6.25	12.5	50	>50	12.5	25	>200
11	3.125	1.56	3.125	12.5	>50	6.25	6.25	>200
12	1.56	1.56	1.56	6.25	>50	3.125	3.125	>200
13	1.56	1.56	1.56	>50	>50	>50	25	>200
14	3.125	0.78	6.25	>50	>50	>50	>50	>200
15	3.125	3.125	1.56	12.5	>50	6.25	6.25	>200
16	3.125	1.56	1.56	6.25	>50	3.125	3.125	>200
17	6.25	6.25	6.25	25	>50	12.5	12.5	119.4 \pm 2.9
18	6.25	6.25	6.25	>50	>50	50	25	88.7 \pm 4.4
19	6.25	6.25	6.25	50	>50	>50	>50	>200
VAN ^b	0.78	1.56	1.56	>50	>50	50	>50	ND ^a
CIP ^c	0.39	0.39	0.39	0.049	0.195	0.39	0.78	ND ^a

^aNot determined. ^bVAN = vancomycin. ^cCIP = ciprofloxacin.

Table 2. Antibacterial and Hemolytic Activities of Compounds 9–19 Combined with 12.5 $\mu\text{g/mL}$ Zn^{2+}

compd with 12.5 $\mu\text{g/mL}$ Zn^{2+}	MIC ($\mu\text{g/mL}$)							HC_{50} ($\mu\text{g/mL}$)
	<i>S. aureus</i> ATCC 29213	MRSA N315	MRSA NCTC10442	<i>E. coli</i> ATCC25922	<i>P. aeruginosa</i> ATCC9027	<i>A. baumannii</i> ATCC17978	<i>A. baumannii</i> R2889	
9	6.25	6.25	12.5	>50	12.5	50	>50	>200
10	3.125	1.56	6.25	50	12.5	12.5	25	>200
11	0.78	0.78	1.56	6.25	6.25	3.125	6.25	>200
12	1.56	0.78	0.78	1.56	6.25	3.125	3.125	>200
13	1.56	0.78	1.56	3.125	>50	>50	25	>200
14	3.125	0.78	6.25	>50	>50	12.5	>50	>200
15	1.56	1.56	0.78	3.125	12.5	3.125	3.125	>200
16	1.56	0.78	1.56	1.56	3.125	0.78	1.56	>200
17	6.25	6.25	6.25	25	>50	12.5	12.5	119.4 \pm 2.9
18	6.25	6.25	6.25	50	>50	50	25	88.7 \pm 4.4
19	3.125	3.125	6.25	>50	>50	>50	>50	>200
VAN ^a	0.78	1.56	1.56	>50	>50	50	>50	ND ^b
CIP ^c	0.39	0.39	0.39	0.049	0.195	0.39	0.78	ND ^b

^aVAN = vancomycin. ^bNot determined. ^cCIP = ciprofloxacin.

Gram-negative bacteria, especially *P. aeruginosa* ATCC9027. To investigate the effect of different hydrophobicities on antibacterial and hemolytic activities, dipicolylamine-containing compounds 10–16 were synthesized, in which the alkyl chain was varied ($\text{R} = -\text{CH}_3$, $-\text{C}_3\text{H}_7$, $-\text{C}_5\text{H}_{11}$, $-\text{C}_7\text{H}_{15}$, $-\text{C}_9\text{H}_{19}$, isoprenyl group, and $-\text{C}_4\text{H}_6\text{F}_3$). Compound 9 without alkyl chains was also prepared. As shown in Tables 1 and 2 and Table S1, compound 9 without alkyl chains showed poor antibacterial activity against both Gram-positive bacteria (MICs = 25 $\mu\text{g/mL}$) and Gram-negative bacteria (MICs ≥ 50 $\mu\text{g/mL}$) and very poor hemolytic activity ($\text{HC}_{50} > 200$ $\mu\text{g/mL}$). When combined with Zn^{2+} (6.25 or 12.5 $\mu\text{g/mL}$), the antibacterial activity of compound 9 was increased 1–4 times. Compound 10, which was incorporated with a

short lipophilic alkyl chain ($\text{R} = -\text{CH}_3$), displayed stronger antibacterial activity than compound 9. The MIC values of compound 10 against Gram-positive bacteria were in the range of 6.25–12.5 $\mu\text{g/mL}$, which were 2- to 4-fold reduced (1.56–6.25 $\mu\text{g/mL}$) after the addition of Zn^{2+} (6.25 or 12.5 $\mu\text{g/mL}$). However, its antibacterial activity against Gram-negative bacteria was still weak. Compounds 11–16 with increased lipid chains exhibited excellent antibacterial activity against Gram-positive bacteria (MICs = 0.78–6.25 $\mu\text{g/mL}$), and their anti-Gram-positive bacterial activity could be further increased by 1–2 times in the presence of Zn^{2+} . Compounds 11–16 displayed very poor antibacterial activity against *P. aeruginosa* (MICs > 50 $\mu\text{g/mL}$). However, compounds 11–12 and 15–16 showed good activity (MICs = 3.125–12.5 $\mu\text{g/mL}$) against

Table 3. MIC Values ($\mu\text{g/mL}$) of Compound 16 in the Presence of Various Concentrations of Zn^{2+}

concentrations of Zn^{2+} ($\mu\text{g/mL}$)	MIC ($\mu\text{g/mL}$)			
	<i>E. coli</i> ATCC25922	<i>P. aeruginosa</i> ATCC9027	MRSA NCTC10442	<i>S. aureus</i> ATCC29213
50	1.56	3.125	0.78	0.78
25	1.56	3.125	0.78	1.56
12.5	1.56	3.125	0.78	1.56
6.25	1.56	3.125	0.78	1.56
3.125	3.125	12.5	1.56	3.125
1.56	6.25	50	1.56	3.125
0.78	6.25	>50	1.56	3.125
0.39	6.25	>50	1.56	3.125
control ^a	6.25	>50	1.56	3.125

^aTreatment with compound 16 only.

Gram-negative bacteria (*E. coli* and *A. baumannii*). Compounds 13–14 containing longer lipid chains ($R = -\text{C}_7\text{H}_{15}$ and $-\text{C}_9\text{H}_{19}$) displayed obviously significantly reduced activity against *E. coli* and *A. baumannii*, with MIC values of ≥ 25 and $>50 \mu\text{g/mL}$, respectively.

However, after chelating with Zn^{2+} , the antibacterial activity of compounds 9–12 and 15–16 against *P. aeruginosa* ATCC9027 was significantly improved from MICs of $>50 \mu\text{g/mL}$ to MICs of 3.125–12.5 $\mu\text{g/mL}$. When combined with Zn^{2+} (6.25 or 12.5 $\mu\text{g/mL}$), the antibacterial activity of compound 16 against *E. coli* and *A. baumannii* was also 2–4 times increased compared with that without Zn^{2+} . Compound 14 with the longest lipophilic chain showed poor activity against Gram-negative bacteria, and its MIC values remained almost the same after the addition of Zn^{2+} . This result indicated that an excessively long lipophilic alkyl chain was detrimental to the biological activity of carbazole derivatives because an excessively long lipophilic alkyl chain would destroy the hydrophilic and hydrophobic balance of the amphiphilic carbazole compounds, resulting in reduced antibacterial activity. Compound 12 containing an *n*-pentyl group and compound 16 containing an isoprenyl group displayed the most promising antibacterial activity against Gram-positive and Gram-negative (except *P. aeruginosa*) bacteria (MICs = 1.56–6.25 $\mu\text{g/mL}$), suggesting that a medium-length alkyl chain was conducive to the balance of hydrophilicity and hydrophobicity of carbazole derivatives, leading to a significant increase in antibacterial activity. When combined with Zn^{2+} (6.25 or 12.5 $\mu\text{g/mL}$), compound 16 with an isoprenyl group showed the best antibacterial activity against both Gram-positive (MICs = 0.78–1.56 $\mu\text{g/mL}$) and Gram-negative bacteria (MICs = 0.78–3.125 $\mu\text{g/mL}$) among all synthesized carbazole compounds. Notably, compound 16 combined with Zn^{2+} also displayed potent antibacterial activity against *P. aeruginosa* (MIC = 3.125 $\mu\text{g/mL}$). These results indicated that the incorporation of an isoprenyl group was conducive to the enhancement of the antibacterial activity of dipicolylamine-containing carbazole derivatives, whether complexed with Zn^{2+} . In our previous reports, the isoprenyl group was also considered to be the best hydrophobic alkane chain for enhancing the interaction between the modified amphiphilic compounds and the phospholipid layer of the bacterial cell membranes.²⁹

To study the effect of different cationic groups on the antibacterial and hemolytic activity, compounds 16–19 containing the same hydrophobic chain of the isoprenyl group were designed and synthesized. As shown in Table 1, compounds 16–19 had good antibacterial activity against

Gram-positive bacteria (MICs = 1.56–6.25 $\mu\text{g/mL}$). However, compounds 17–19 displayed weak or poor antibacterial activity against Gram-negative bacteria. After the addition of 6.25–12.5 $\mu\text{g/mL}$ Zn^{2+} , their antibacterial activities were not changed (Table 2 and Table S1). The reason for this could be that the cationic moieties of compounds 17–19 were incapable of chelating with Zn^{2+} . Only compound 16 showed good antibacterial activity against the *E. coli* and *A. baumannii* strains tested, with MICs of 3.125–6.25 $\mu\text{g/mL}$. Notably, the antibacterial activity of compound 16 against both Gram-positive and Gram-negative bacteria was greatly enhanced after the addition of 6.25–12.5 $\mu\text{g/mL}$ Zn^{2+} , including *P. aeruginosa* ATCC9027, with MICs of 0.78–3.125 $\mu\text{g/mL}$.

Effect of Various Concentrations of Zn^{2+} on the Activity of 16. The effect of different concentrations of Zn^{2+} on the antibacterial activity of compound 16 was explored. As shown in Table 3, when the added concentration of Zn^{2+} was more than 3.125 $\mu\text{g/mL}$, an obvious increase in antibacterial activity was observed. When the added concentration of Zn^{2+} was less than 3.125 $\mu\text{g/mL}$, the MIC values remained unchanged. These results indicated that the incorporation of a dipicolylamine group as the cationic moiety would significantly enhance the antibacterial activity of carbazole compounds against both Gram-positive and Gram-negative bacteria in the presence of Zn^{2+} .

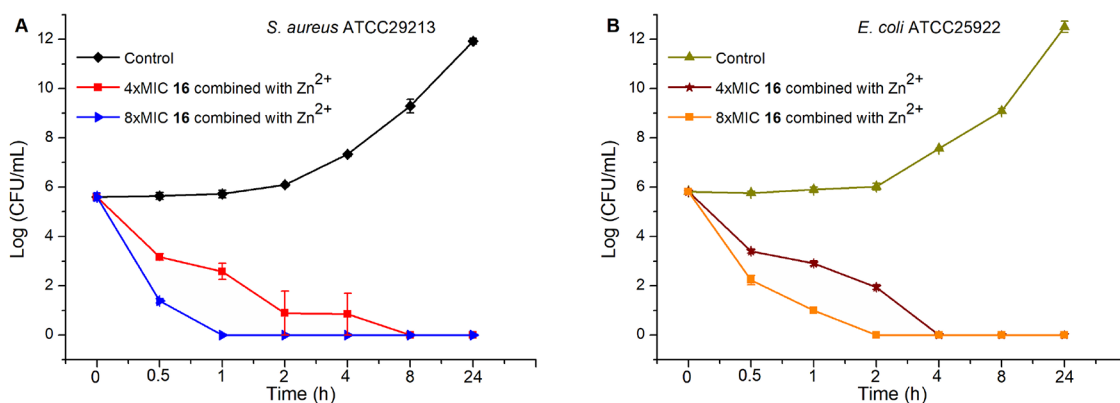
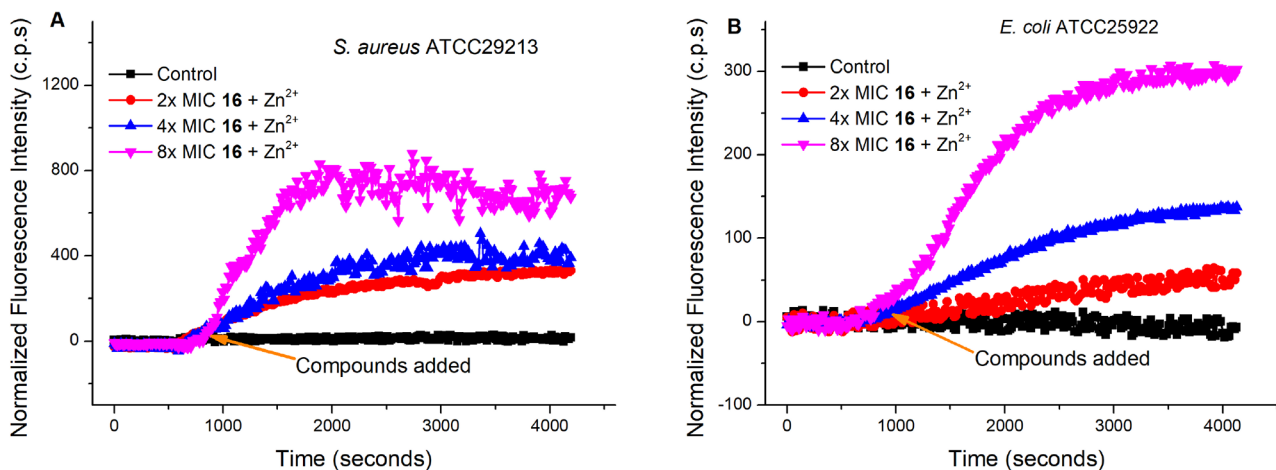
After preliminary structure–activity relationship study, we found that the incorporation of dipicolylamine can form a Zn-DPA complex in the presence of Zn^{2+} and then could efficiently interact with the negatively charged bacterial membranes of Gram-positive and Gram-negative bacteria through electrostatic interaction. Among all the lipid chains investigated, the introduction of isoprenyl group is more conducive to improving the antibacterial activity. This finding is consistent with our earlier studies.^{29,43} The reason may be that the isoprenyl group can promote the insertion of the amphiphilic carbazole derivatives into the phospholipid bilayer of bacterial membrane more efficiently through hydrophobic interaction. So far, this study has illustrated the strategy of designing and synthesizing a series of carbazole-based CAMPs mimics as broad-spectrum antibacterial agents. Their activities are determined by several structural parameters, including amphiphilicity, positive charge of cationic groups, and hydrophobic lipid chains.

In Vitro Salt Resistance Study. The stability of compound 16 combined with 12.5 $\mu\text{g/mL}$ Zn^{2+} in the presence of various salt conditions was evaluated by determining the MIC changes. Compound 16 combined with 12.5 $\mu\text{g/mL}$ Zn^{2+} was incubated with bacterial

Table 4. MIC Values ($\mu\text{g/mL}$) of Compound 16 Combined with $12.5 \mu\text{g/mL Zn}^{2+}$ under Physiological Concentrations of Various Salts

condition	MIC ($\mu\text{g/mL}$)				
	<i>S. aureus</i> ATCC29213	MRSA N315	MRSA NCTC10442	<i>E. coli</i> ATCC25922	<i>A. baumannii</i> ATCC17978
control ^a	1.56	0.78	1.56	1.56	0.78
3220 $\mu\text{g/mL Na}^+$	1.56	0.78	1.56	3.125	0.78
175.5 $\mu\text{g/mL K}^+$	1.56	0.78	1.56	1.56	0.78
100 $\mu\text{g/mL Ca}^{2+}$	3.125	3.125	3.125	6.25	3.125
24.3 $\mu\text{g/mL Mg}^{2+}$	1.56	1.56	1.56	3.125	1.56

^aTreatment with compound 16 combined with $12.5 \mu\text{g/mL Zn}^{2+}$ only.

**Figure 2.** Bacterial killing kinetics of compound 16 combined with $12.5 \mu\text{g/mL Zn}^{2+}$ against *S. aureus* ATCC29213 (A) and *E. coli* ATCC25922 (B). Data are presented as means \pm s.d. from two independent experiments.**Figure 3.** Cytoplasmic membrane permeabilization of compound 16 combined with $12.5 \mu\text{g/mL Zn}^{2+}$ against *S. aureus* ATCC29213 (A) and *E. coli* ATCC25922 (B) using a SYTOX-Green assay. The data are representative of two independent experiments.

suspensions (*S. aureus* ATCC29213, MRSA NCTC10442, MRSA N315, *E. coli* ATCC25922, or *A. baumannii* ATCC17978) using Mueller Hinton broth (MHB) containing physiological concentrations of $3220 \mu\text{g/mL Na}^+$, $175.5 \mu\text{g/mL K}^+$, $100 \mu\text{g/mL Ca}^{2+}$, or $24.3 \mu\text{g/mL Mg}^{2+}$, respectively. As shown in Table 4, the MIC values of compound 16 combined with $12.5 \mu\text{g/mL Zn}^{2+}$ under physiological concentrations of Na^+ , K^+ , or Mg^{2+} were almost consistent with the original values (MICs = $0.78\text{--}3.125 \mu\text{g/mL}$). After the addition of $100 \mu\text{g/mL Ca}^{2+}$, compound 16 combined with $12.5 \mu\text{g/mL Zn}^{2+}$ maintained its potent antibacterial activity, with MIC values of $3.125\text{--}6.25 \mu\text{g/mL}$. However, the MIC values of compound 16 combined with $12.5 \mu\text{g/mL Zn}^{2+}$ in the presence of $100 \mu\text{g/mL Ca}^{2+}$ were 1- to 2-fold reduced compared with their

original values. These results demonstrated that compound 16 combined with $12.5 \mu\text{g/mL Zn}^{2+}$ had very high salt resistance on the antibacterial activity and could overcome the instability issue associated with CAMPs at physiological salt concentrations.

Bacterial Killing Kinetic Evaluation. The bacterial killing kinetics of the most promising compound 16 combined with Zn^{2+} were evaluated against *S. aureus* ATCC29213 and *E. coli* ATCC25922. A suspension of *S. aureus* ATCC29213 or *E. coli* ATCC25922 was incubated with different concentrations of compound 16 (4 \times and 8 \times MIC) combined with $12.5 \mu\text{g/mL Zn}^{2+}$ at 37°C . As shown in Figure 2, 4 \times MIC compound 16 combined with $12.5 \mu\text{g/mL Zn}^{2+}$ obtained a 3.03 log reduction in the bacterial counts of *S. aureus* ATCC29213 and a 2.91 log

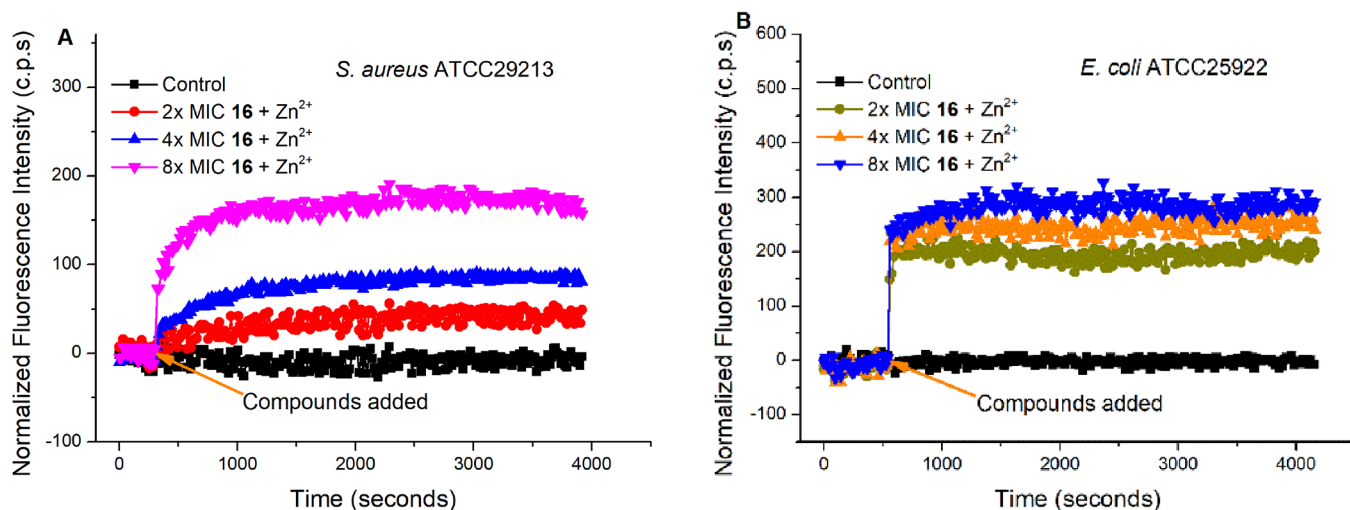


Figure 4. Membrane depolarization against *S. aureus* ATCC29213 (A) and *E. coli* ATCC25922 (B) using DiSC₃ (S) dye as a fluorescence probe. The data are representative of two independent experiments.

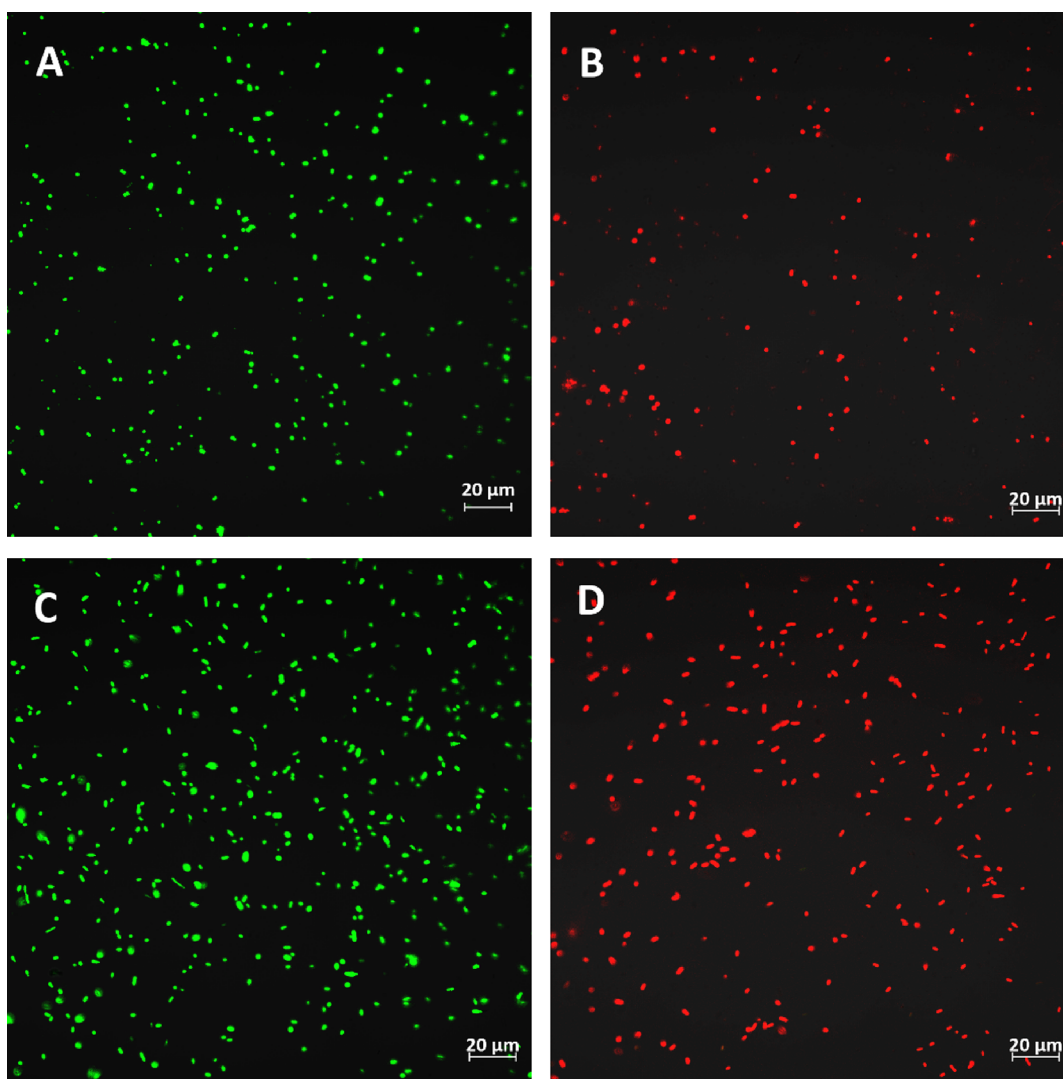


Figure 5. Fluorescence image of *S. aureus* ATCC29213 or *E. coli* ATCC25922 cells stained with SYTO 9 and propidium iodide after treatment with PBS or 8x MIC compound 16 combined with 12.5 μg/mL Zn²⁺: (A) PBS-treated *S. aureus* ATCC29213 cells, (B) compound 16 combined with 12.5 μg/mL Zn²⁺-treated *S. aureus* ATCC29213 cells; (C) PBS-treated *E. coli* ATCC25922 cells, (D) compound 16 combined with 12.5 μg/mL Zn²⁺-treated *E. coli* ATCC25922 cells. The figures are representative of two independent experiments.

reduction in the bacterial counts of *E. coli* ATCC25922 within 1 h. Additionally, 8× MIC compound **16** combined with 12.5 μg/mL Zn²⁺ achieved a more than 3 log reduction in the bacterial counts of both *S. aureus* ATCC29213 (4.22 log) and *E. coli* ATCC25922 (3.59 log) within 0.5 h. These results indicated that compound **16** combined with Zn²⁺ displayed a rapid bactericidal property. This rapid bactericidal property is beneficial to shorten the treatment time of infectious diseases and reduce the probability of drug resistance.

Antibacterial Mechanism Studies (Disruption of Bacterial Cell Membrane Integrity). Because compound **16** combined with 12.5 μg/mL Zn²⁺ showed the best *in vitro* antibacterial activity, very low hemolytic activity, rapid bactericidal property, and high salt resistance, we used compound **16** combined with 12.5 μg/mL Zn²⁺ to explore the antibacterial mechanism. Most antimicrobial peptidomimetics were reported to act on bacteria via a membrane-disruptive mechanism.^{24,25} To study the mode of action for compound **16** combined with 12.5 μg/mL Zn²⁺ against both Gram-positive and Gram-negative bacteria, we used various fluorescent probes, including SYTOX Green, DiSC₃ (5), SYTO 9, propidium iodide (PI), 1-*N*-phenyl-naphthylamine (NPN), and BODIPY-TR-cadaverine.

Cytoplasmic Membrane Permeabilization. SYTOX Green dye is commonly used to measure the integrity of bacterial cell membranes. SYTOX Green cannot pass through intact cell membranes but can enter disrupted cell membranes and combine with intracellular nucleic acids to significantly enhance fluorescence.⁶¹ The effect of compound **16** in the presence of 12.5 μg/mL Zn²⁺ on the permeabilization of bacterial cell membranes was evaluated by measuring the change in fluorescence. As shown in Figure 3, when compound **16** combined with 12.5 μg/mL Zn²⁺ was added to SYTOX Green-treated *S. aureus* ATCC29213 or *E. coli* ATCC25922, a significant increase in fluorescence intensity was observed in an obvious concentration-dependent manner. The results demonstrated that compound **16** combined with 12.5 μg/mL Zn²⁺ killed both Gram-positive and Gram-negative bacteria by destroying the integrity of the bacterial cell membranes in a concentration-dependent manner.

Cytoplasmic Membrane Depolarization Ability. To further verify the membrane-targeting mechanism of compound **16** combined with 12.5 μg/mL Zn²⁺, DiSC₃ (5) was used to evaluate its effect on the depolarization of bacterial cell membranes. DiSC₃ (5), as a membrane potential-sensitive probe, accumulated in the phospholipid bilayer and then self-quenched; when the membrane potential was changed, the fluorescence intensity sharply increased.⁶² As shown in Figure 4, after compound **16** combined with 12.5 μg/mL Zn²⁺ was added to the DiSC₃ (5)-treated Gram-positive bacterium *S. aureus* ATCC29213 or Gram-negative bacterium *E. coli* ATCC25922, a significant increase in fluorescence intensity was observed. These results indicated that the membrane potential of the bacterial cell membranes was depolarized by compound **16** combined with 12.5 μg/mL Zn²⁺, demonstrating that compound **16** combined with 12.5 μg/mL Zn²⁺ acted on both Gram-positive and Gram-negative bacteria via a membrane targeting mode of action.

Membrane Integrity Analysis. A LIVE/DEAD BacLight bacterial viability kit L7007 composed of SYTO 9 and PI was used to measure the membrane integrity of bacterial cells. Bacterial cells with damaged membranes will be stained red, while bacterial cells with intact membranes will be stained

green.⁶³ The bacterial suspensions of *S. aureus* ATCC29213 or *E. coli* ATCC25922 were mixed with 8× MIC compound **16** combined with 12.5 μg/mL Zn²⁺ or PBS (negative control). After 2 h of incubation at 37 °C, these bacterial cells were stained with PI and SYTO 9. As shown in Figure 5, both *S. aureus* ATCC29213 and *E. coli* ATCC25922 cells treated with compound **16** combined with 12.5 μg/mL Zn²⁺ were stained with strong red fluorescence and negligible green fluorescence, suggesting that the membrane integrity of both *S. aureus* ATCC29213 and *E. coli* ATCC25922 cells had been obviously damaged. The PBS-treated groups were stained with only strong green fluorescence, indicating that bacterial membranes were intact. These results demonstrated that compound **16** combined with 12.5 μg/mL Zn²⁺ effectively acted on both Gram-positive and Gram-negative bacteria by destroying the integrity of the bacterial membranes.

Outer Membrane Permeability. The hydrophobic fluorescent probe NPN is commonly used to explore the interactions of antimicrobial agents with the outer membranes of Gram-negative bacteria (e.g., *E. coli*). NPN cannot pass through the intact outer membranes of bacterial cells, but when the outer membranes of bacterial cells are damaged, NPN can freely enter the phospholipid layer and cause a significant increase in fluorescence intensity.⁶⁴ As shown in Figure 6, after compound **16** combined with 12.5 μg/mL Zn²⁺

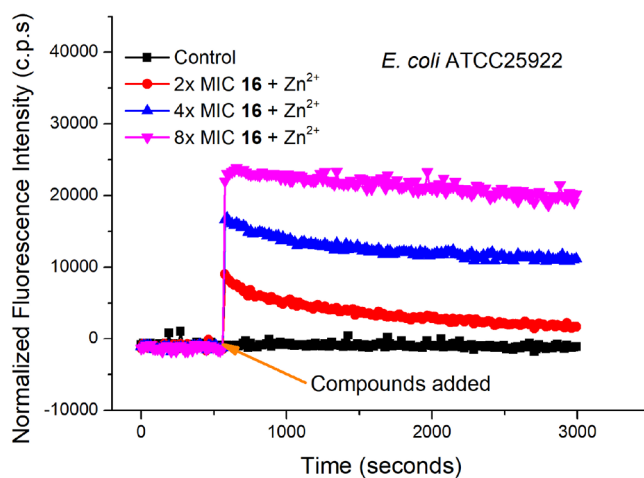


Figure 6. Outer membrane permeabilization of compound **16** combined with 12.5 μg/mL Zn²⁺ against *E. coli* ATCC25922 using the probe 1-*N*-phenyl-naphthylamine. The data are representative of two independent experiments.

was added to NPN-treated *E. coli* ATCC25922, a significant increase in fluorescence intensity was observed. This result revealed that compound **16** in the presence of 12.5 μg/mL Zn²⁺ can penetrate and destroy the outer membranes of *E. coli* in a concentration-dependent manner, demonstrating that compound **16** combined with 12.5 μg/mL Zn²⁺ exerted an antibacterial effect against Gram-negative bacteria through a membrane-targeting mode of action.

LPS Binding. The binding affinity between compound **16** combined with 12.5 μg/mL Zn²⁺ and LPS was investigated by determining the displacement of BODIPY-TR-cadaverine bonded to LPS. When the probe was bonded to LPS, quenching of the fluorescence intensity was observed, but when the probe was replaced and redissolved in solution, a significant increase in fluorescence was observed.^{65,66} As shown

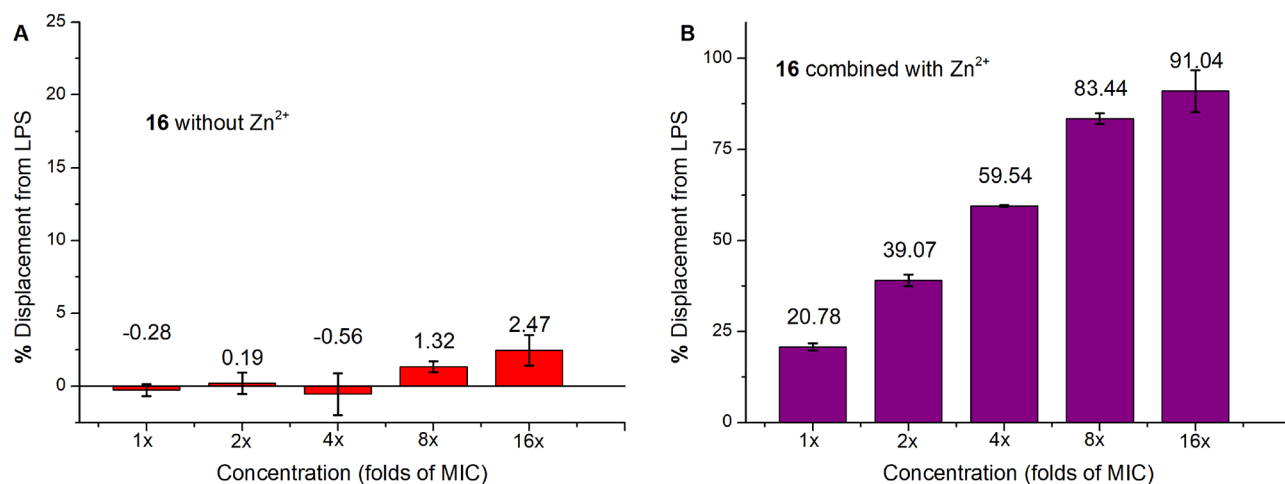


Figure 7. Determination of BODIPY-TR-cadaverine displacement from lipopolysaccharides (LPS) by compound **16** without Zn²⁺ (A) or combined with 12.5 µg/mL Zn²⁺ (B). BODIPY-TR-cadaverine displacement from LPS was calculated using the formula below: % Displacement from LPS = $[(F_{\text{compound}} - F_{\text{blank}})/(F_{\text{max}} - F_{\text{blank}})] \times 100$, where F_{blank} is the fluorescence intensity of BODIPY-TR-cadaverine with only LPS, and F_{max} is the fluorescence intensity of BODIPY-TR-cadaverine without LPS and compounds. Data are presented as means \pm s.d. from two independent experiments.

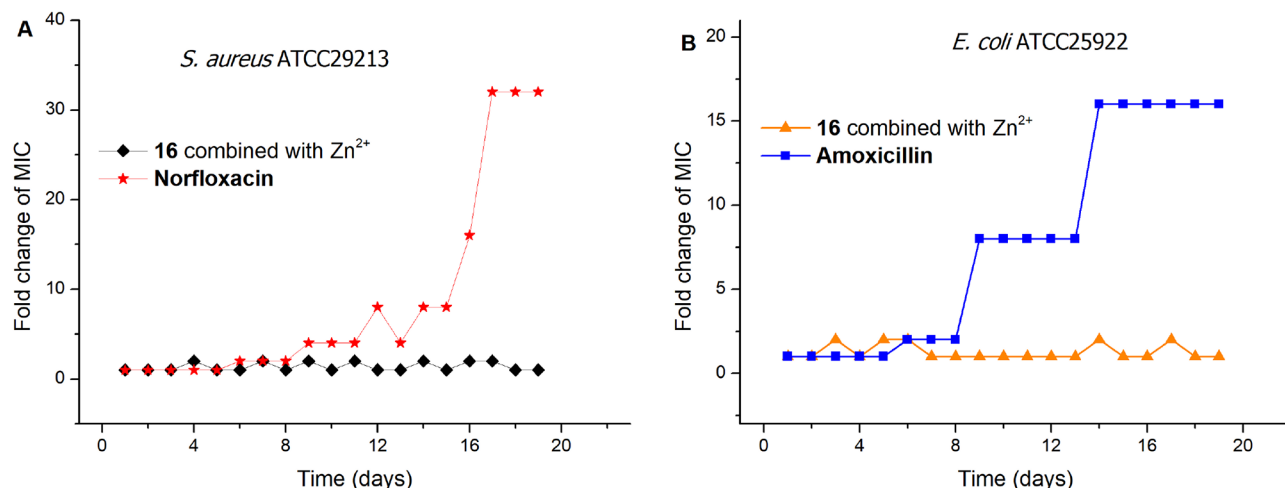


Figure 8. Bacterial resistance studies of compound **16** combined with 12.5 µg/mL Zn²⁺ against *S. aureus* ATCC29213 (A) and *E. coli* ATCC25922 (B). Norfloxacin and amoxicillin were selected as comparisons for *S. aureus* ATCC29213 and *E. coli* ATCC25922, respectively. The data are representative of two independent experiments.

in Figure 7, BODIPY-TR-cadaverine displacement from LPS by compound **16** combined with 12.5 µg/mL Zn²⁺ was significantly increased compared with that of compound **16** without Zn²⁺. The BODIPY-TR-cadaverine displacement from LPS by 1× MIC compound **16** combined with 12.5 µg/mL Zn²⁺ was 20.78 \pm 1.03%. However, when the concentration of compound **16** was increased to 16× MIC (combined with 12.5 µg/mL Zn²⁺), BODIPY-TR-cadaverine displacement from LPS was greatly enhanced (91.04 \pm 5.77%), indicating that the interaction between LPS and compound **16** combined with 12.5 µg/mL Zn²⁺ was strong and concentration-dependent. However, compound **16** without Zn²⁺ showed a very weak affinity for LPS, which was in accordance with its poor anti-Gram-negative bacterial activity. These results proved that the addition of Zn²⁺ can cause a strong interaction between compound **16** and the LPS of Gram-negative bacteria, and then compound **16** combined with Zn²⁺ could pass through the LPS layer to interact with the bacterial membranes of

Gram-negative bacteria, leading to the destruction of bacterial cell membrane integrity and bacterial death.

Tendency to Develop Bacterial Resistance. The development of antibiotic resistance has become a crucial evaluation factor for the discovery and development of new antibiotics.² Compound **16** combined with 12.5 µg/mL Zn²⁺ was selected to evaluate drug resistance development toward *S. aureus* and *E. coli*, using multipassage resistance selection studies.^{43,67} Compound **16** combined with 12.5 µg/mL Zn²⁺ or norfloxacin was continuously exposed to *S. aureus* ATCC29213 at subinhibitory concentrations of antimicrobials. As shown in Figure 8A, after 19 days, the fold change of MICs of compound **16** combined with 12.5 µg/mL Zn²⁺ against *S. aureus* ATCC29213 remained unchanged and stable, suggesting that compound **16** combined with 12.5 µg/mL Zn²⁺ can effectively avoid the development of bacterial resistance. After 17 days, the fold change in the MICs of norfloxacin was increased by 32-fold, indicating that the bacterial resistance development induced by norfloxacin was significant. The drug

resistance of *E. coli* ATCC25922 to compound **16** combined with 12.5 $\mu\text{g/mL}$ Zn^{2+} or amoxicillin during serial passaging in the presence of subinhibitory concentrations of antimicrobials is displayed in Figure 8B, after 15 days, the MIC value of amoxicillin increased to 16-fold, suggesting that the bacterial resistance caused by amoxicillin was obvious. By contrast, after 19 days, the antibacterial potency against *E. coli* ATCC25922 of compound **16** combined with 12.5 $\mu\text{g/mL}$ Zn^{2+} was unaltered, indicating that compound **16** combined with 12.5 $\mu\text{g/mL}$ Zn^{2+} can effectively prevent resistance development. The avoidance of bacterial resistance was one of the advantages of compound **16** combined with Zn^{2+} over commercial antibiotics and might be associated with its membrane-active mode of action.

In Vitro Cytotoxicity Evaluation. The *in vitro* cytotoxicity of compound **16** combined with 12.5 $\mu\text{g/mL}$ Zn^{2+} toward mammalian cells was determined using a CCK-8 assay.⁴³ As shown in Figure 9, even with compound **16** in the presence of

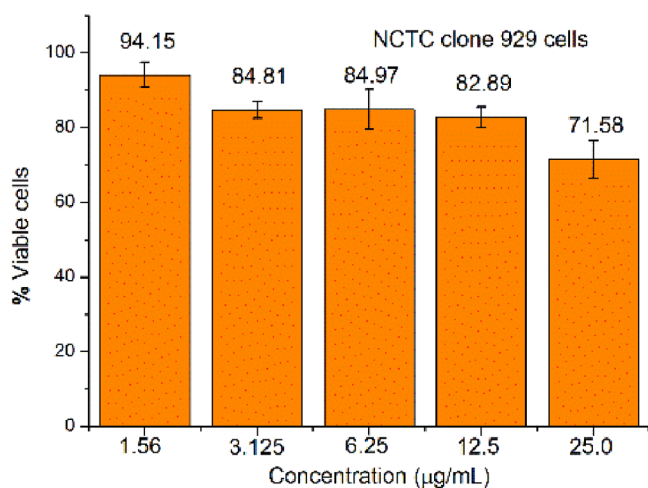


Figure 9. Cytotoxicity of compound **16** combined with 12.5 $\mu\text{g/mL}$ Zn^{2+} toward mouse fibroblasts (NCTC clone 929).

12.5 $\mu\text{g/mL}$ Zn^{2+} at the highest tested concentration of 25 $\mu\text{g/mL}$ (16–32 \times MIC), the cell survival percentage of mouse

fibroblasts (NCTC clone 929) was maintained at $71.58 \pm 5.01\%$. This result indicated that compound **16** in the presence of 12.5 $\mu\text{g/mL}$ Zn^{2+} had very low cytotoxicity toward mammalian cells.

In Vivo Antibacterial Efficacy. Finally, the therapeutic potential of compound **16** combined with Zn^{2+} as a broad-spectrum antimicrobial agent was evaluated using a murine bacterial keratitis model induced by *S. aureus* ATCC29213 or *P. aeruginosa* ATCC9027. In the *S. aureus* ATCC29213-induced corneal infection model, the mice were immunosuppressed by intraperitoneal injections of cyclophosphamide (100 mg/kg) three times 5 days before infection. One day after infection, each group of mice ($n = 5$) was topically treated with 0.5% compound **16** combined with 12.5 $\mu\text{g/mL}$ Zn^{2+} , 5% vancomycin (positive control), or 5% glucose solution (negative control) four times daily for 3 days. As shown in Figure 10A, compared with the negative group, the count of viable bacteria in the infected cornea for 0.5% compound **16** combined with Zn^{2+} and 5% vancomycin were reduced by 6.5 log ($p < 0.005$) and 5.4 log ($p < 0.005$), respectively. This result suggested that compound **16** in the presence of 12.5 $\mu\text{g/mL}$ Zn^{2+} had excellent *in vivo* efficacy against *S. aureus* ATCC29213, and its efficacy was superior to that of vancomycin.

In the *P. aeruginosa* ATCC9027-induced keratitis model, the mice were not immunosuppressed, and 0.3% gatifloxacin was used as a positive control. As shown in Figure 10B, compared with the negative group, 0.5% compound **16** combined with 12.5 $\mu\text{g/mL}$ Zn^{2+} and 0.3% gatifloxacin reduced the count of viable bacteria in the infected cornea by 4.46 log ($p < 0.02$) and 3.03 log ($p < 0.02$), respectively. This result indicated that 0.5% compound **16** combined with 12.5 $\mu\text{g/mL}$ Zn^{2+} had better *in vivo* efficacy against *P. aeruginosa* ATCC9027 than 0.3% gatifloxacin. *In vivo* efficacy studies demonstrated that compound **16** combined with Zn^{2+} holds great potential as an effective broad-spectrum antimicrobial agent for the treatment of bacterial infections caused by both Gram-positive and Gram-negative bacteria.

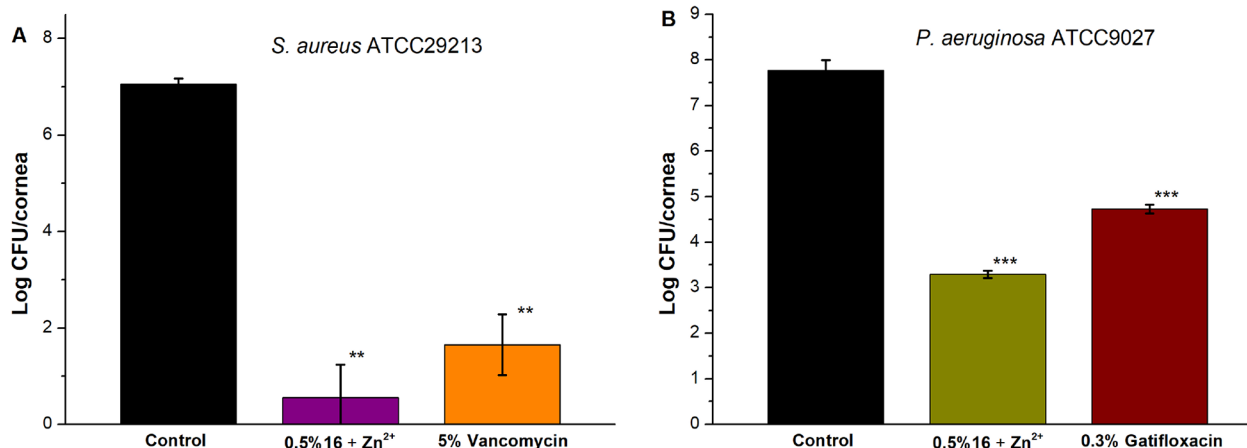


Figure 10. *In vivo* antibacterial efficacy of compound **16** combined with 12.5 $\mu\text{g/mL}$ Zn^{2+} in a murine keratitis model induced by *S. aureus* ATCC29213 or *P. aeruginosa* ATCC9027 ($n = 5$). Vancomycin (5%) or gatifloxacin (0.3%) was selected as the positive control, and 5% glucose solution was used as a negative control. (**) $P < 0.005$ and (***) $P < 0.02$ compared with the negative control. The results are given as means \pm s.d. for five mice.

CONCLUSIONS

In this work, we rationally designed and synthesized a novel series of dipicolylamine-containing cationic carbazole amphiphiles by biomimicking CAMPs. After performing biological activity evaluations and structural optimization, compound **16** was identified as the most promising antimicrobial candidate. Compound **16** combined with Zn^{2+} (6.25–12.5 $\mu\text{g}/\text{mL}$) showed potent broad-spectrum antibacterial activity against both Gram-positive and Gram-negative bacteria (MICs = 0.78–3.125 $\mu\text{g}/\text{mL}$). The addition of Zn^{2+} greatly improved the antibacterial activity of compound **16** against both Gram-positive and Gram-negative bacteria, especially *P. aeruginosa* ATCC9027 (MIC from >50 to 3.125 $\mu\text{g}/\text{mL}$). The mode of action studies revealed that compound **16** combined with Zn^{2+} killed both Gram-positive and Gram-negative bacteria mainly by affecting the permeability of bacterial cell membranes or even disrupting the integrity of bacterial cell membranes. Compound **16** combined with 12.5 $\mu\text{g}/\text{mL}$ Zn^{2+} had very poor hemolytic activity ($\text{HC}_{50} > 200 \mu\text{g}/\text{mL}$) as well as low cytotoxicity toward mammalian cells and could avoid the emergence of bacterial resistance in the laboratory simulation of drug resistance development studies. More notably, compound **16** combined with 12.5 $\mu\text{g}/\text{mL}$ Zn^{2+} displayed excellent *in vivo* efficacy in a murine keratitis model induced by *S. aureus* ATCC29213 or *P. aeruginosa* ATCC9027, and the *in vivo* efficacy of compound **16** combined with Zn^{2+} was superior to that of commercial vancomycin and gatifloxacin. This work presents a framework for the design and synthesis of a new generation of membrane-active antimicrobials to combat Gram-positive and Gram-negative bacterial infections.

EXPERIMENTAL SECTION

General Chemistry. All commercial chemicals and solvents were used without further purification. NMR spectra were recorded on a JEOL 400 MHz spectrometer. Chemical shifts and coupling constants are expressed in ppm and Hz, respectively. HPLC was carried out on an Agilent 1260 Infinity system by using YMC-Pack C18 column (20 \times 150 mm or 20 \times 100 mm, 5 μm , 120 \AA) and gradient elution mode. The following mobile phases were applied: buffer A: 0.1% HCOOH in water; buffer B: 0.1% HCOOH in methanol. All final products were purified to more than 95% purity. High-resolution mass (HRMS) spectra were performed with a Thermo DFS mass spectrometer.

Synthesis of Carbazole Derivatives. The synthesis of carbazole derivatives **2–6**, **8**, and **17–18** was described previously.⁴³

9-(4,4,4-Trifluorobutyl)-4-(oxiran-2-ylmethoxy)-9H-carbazole (7). NaOH (53 mg, 0.66 mmol) and 1,1,1-trifluoro-4-iodobutane (109 μL , 0.67 mmol) were added to a solution of **1** (100 mg, 0.42 mmol) in DMF (5 mL). The mixture was stirred for 2 h at 60 $^{\circ}\text{C}$. Then, the mixture was diluted with ethyl acetate and extracted with water three times. The organic phase was concentrated under reduced pressure. The crude product was purified by silica gel chromatography (ethyl acetate/petroleum ether = 1/4) to give **7** as a light yellow solid (103.2 mg, 71%); mp 75.8–78.3 $^{\circ}\text{C}$. ^1H NMR (400 MHz, CDCl_3) δ 8.38 (d, J = 7.3 Hz, 1H), 7.58–7.26 (m, 4H), 7.02 (d, J = 7.7 Hz, 1H), 6.69 (d, J = 7.7 Hz, 1H), 4.53–4.21 (m, 4H), 3.71–3.37 (m, 1H), 2.96 (d, J = 43.3 Hz, 2H), 2.18–2.02 (m, 4H). ^{13}C NMR (100 MHz, CDCl_3) δ 155.24, 141.78, 139.47, 126.75, 125.56, 125.22, 123.55, 122.31, 119.69, 112.35, 107.89, 101.94, 101.31, 68.91, 50.45, 44.96, 41.86, 31.64, 21.80. HRMS (ESI+): calculated for $\text{C}_{19}\text{H}_{19}\text{F}_3\text{NO}_2$ [$\text{M} + \text{H}$]⁺ 350.1368, found 350.1354. HPLC purity: 99.5%, t_{R} = 6.4 min.

1-((9H-Carbazol-4-yl)oxy)-3-(bis(pyridin-2-ylmethyl)amino)propan-2-ol (9). 2,2'-Dipicolylamine (0.2 mL) was added to a solution of **1** (100 mg, 0.37 mmol) in MeOH (10 mL). The mixture was stirred at 65 $^{\circ}\text{C}$ for 6 h. After the reaction was completed, the

mixture was diluted with ethyl acetate and washed with water three times. The organic phase was evaporated in vacuum. The resulting residue was purified by HPLC to give **9** as a dark green solid (127.3 mg, 78%); mp 78.6–81.9 $^{\circ}\text{C}$. ^1H NMR (400 MHz, CD_3OD) δ 8.31–8.22 (m, 2H), 7.94 (d, J = 7.8 Hz, 1H), 7.58–7.51 (m, 2H), 7.45 (d, J = 7.8 Hz, 2H), 7.37 (d, J = 8.1 Hz, 1H), 7.31–7.22 (m, 2H), 7.12–6.95 (m, 4H), 6.58 (d, J = 7.7 Hz, 1H), 4.34–4.25 (m, 1H), 4.18 (d, J = 4.0 Hz, 2H), 4.03–3.89 (m, 4H), 3.16–2.93 (m, 2H). ^{13}C NMR (100 MHz, CD_3OD) δ 158.96 (2 \times C), 156.35, 149.07 (2 \times CH), 142.82, 140.59, 138.97 (2 \times CH), 127.37, 125.52, 125.02 (2 \times CH), 123.93 (2 \times CH), 123.91, 123.50, 119.75, 113.57, 111.00, 104.90, 101.25, 70.41, 68.83, 61.36 (2 \times CH_2), 58.47. HRMS (ESI+): calculated for $\text{C}_{27}\text{H}_{27}\text{N}_4\text{O}_2$ [$\text{M} + \text{H}$]⁺ 439.2134, found 439.2127. HPLC purity: 99.6%, t_{R} = 6.1 min.

1-(Bis(pyridin-2-ylmethyl)amino)-3-((9-methyl-9H-carbazol-4-yl)oxy)propan-2-ol (10). **10** was prepared from 2,2'-dipicolylamine (0.2 mL) and **2** (65.9 mg, 0.26 mmol) according to the similar procedure for **9** to give **10** as a dark green solid (87.2 mg, 74%); mp 49.2–51.8 $^{\circ}\text{C}$. ^1H NMR (400 MHz, CDCl_3) δ 8.58 (d, J = 4.1 Hz, 2H), 8.16 (d, J = 7.7 Hz, 1H), 7.65–7.56 (m, 2H), 7.46–7.32 (m, 5H), 7.20–7.11 (m, 3H), 7.02 (d, J = 8.1 Hz, 1H), 6.68 (d, J = 8.0 Hz, 1H), 5.13 (s, 2H), 4.46–4.38 (m, 1H), 4.36–4.19 (m, 2H), 4.12–4.00 (m, 3H), 3.83 (s, 3H), 3.28–3.03 (m, 2H). ^{13}C NMR (100 MHz, CDCl_3) δ 158.72 (2 \times C), 155.33, 148.76 (2 \times CH), 142.55, 140.28, 137.08 (2 \times CH), 126.52, 124.72, 123.48 (2 \times CH), 123.07, 122.45 (2 \times CH), 122.15, 119.15, 111.98, 107.87, 101.64, 100.84, 70.09, 67.96, 60.33, 58.52, 50.84, 29.36. HRMS (ESI+): calculated for $\text{C}_{28}\text{H}_{29}\text{N}_4\text{O}_2$ [$\text{M} + \text{H}$]⁺ 453.2291, found 453.2281. HPLC purity: 99.1%, t_{R} = 6.1 min.

1-(Bis(pyridin-2-ylmethyl)amino)-3-((9-propyl-9H-carbazol-4-yl)oxy)propan-2-ol (11). **11** was synthesized from 2,2'-dipicolylamine (0.2 mL) and **3** (93 mg, 0.33 mmol) according to the similar procedure for **9** to provide **11** as a dark green solid (112.7 mg, 71%); mp 53.1–54.7 $^{\circ}\text{C}$. ^1H NMR (400 MHz, CDCl_3) δ 8.56 (d, J = 4.2 Hz, 2H), 8.14 (d, J = 7.7 Hz, 1H), 7.64–7.52 (m, 2H), 7.45–7.29 (m, 5H), 7.18–7.07 (m, 3H), 7.01 (d, J = 8.2 Hz, 1H), 6.65 (d, J = 8.0 Hz, 1H), 4.43–4.36 (m, 1H), 4.35–4.16 (m, 7H), 4.01 (d, J = 14.9 Hz, 2H), 3.27–2.99 (m, 2H), 1.96–1.80 (m, 2H), 0.95 (t, J = 7.4 Hz, 3H). ^{13}C NMR (100 MHz, CDCl_3) δ 158.62 (2 \times C), 155.39, 148.70 (2 \times CH), 142.07, 139.79, 137.15 (2 \times CH), 126.40, 124.62, 123.54 (2 \times CH), 123.13, 122.49 (2 \times CH), 122.19, 119.03, 112.01, 108.18, 101.97, 100.66, 70.05, 67.95, 60.30 (2 \times CH_2), 58.53, 44.84, 22.39, 11.84. HRMS (ESI+): calculated for $\text{C}_{30}\text{H}_{33}\text{N}_4\text{O}_2$ [$\text{M} + \text{H}$]⁺ 481.2604, found 481.2593. HPLC purity: 98.8%, t_{R} = 5.2 min.

1-(Bis(pyridin-2-ylmethyl)amino)-3-((9-pentyl-9H-carbazol-4-yl)oxy)propan-2-ol (12). **12** was synthesized from 2,2'-dipicolylamine (0.2 mL) and **4** (42.8 mg, 0.14 mmol) according to the similar procedure for **9** to give **12** as a dark green solid (49.3 mg, 70%); mp 56.2–59.1 $^{\circ}\text{C}$. ^1H NMR (400 MHz, CDCl_3) δ 8.59–8.48 (m, 2H), 8.15 (d, J = 7.7 Hz, 1H), 7.63–7.50 (m, 2H), 7.43–7.28 (m, 5H), 7.19–7.06 (m, 3H), 7.01 (d, J = 8.1 Hz, 1H), 6.65 (d, J = 7.9 Hz, 1H), 4.73 (s, 2H), 4.43–4.35 (m, 1H), 4.33–4.16 (m, 4H), 4.10–3.98 (m, 3H), 3.29–2.98 (m, 2H), 1.92–1.76 (m, 2H), 1.40–1.28 (m, 4H), 0.87 (t, J = 7.1 Hz, 3H). ^{13}C NMR (100 MHz, CDCl_3) δ 157.90 (2 \times C), 155.29, 148.38 (2 \times CH), 141.98, 139.70, 137.60 (2 \times CH), 126.43, 124.65, 123.87 (2 \times CH), 123.09, 122.77 (2 \times CH), 122.15, 119.01, 111.96, 108.16, 101.98, 100.63, 69.92, 67.73, 60.00, 58.49, 50.78, 43.28, 29.45, 28.77, 22.57, 14.06. HRMS (ESI+): calculated for $\text{C}_{32}\text{H}_{37}\text{N}_4\text{O}_2$ [$\text{M} + \text{H}$]⁺ 509.2917, found 509.2911. HPLC purity: 99.1%, t_{R} = 7.4 min.

1-(Bis(pyridin-2-ylmethyl)amino)-3-((9-heptyl-9H-carbazol-4-yl)oxy)propan-2-ol (13). **13** was synthesized from 2,2'-dipicolylamine (0.2 mL) and **5** (42.5 mg, 0.13 mmol) according to the similar procedure for **9** to give **13** as a dark green solid (52.2 mg, 77%); mp 61.1–63.5 $^{\circ}\text{C}$. ^1H NMR (400 MHz, CDCl_3) δ 8.60–8.46 (m, 2H), 8.15 (d, J = 7.7 Hz, 1H), 7.63–7.50 (m, 2H), 7.44–7.28 (m, 5H), 7.18–7.06 (m, 3H), 7.00 (d, J = 8.1 Hz, 1H), 6.65 (d, J = 7.9 Hz, 1H), 4.43–4.35 (m, 1H), 4.34–4.16 (m, 4H), 4.09–3.98 (m, 3H), 3.89 (s, 2H), 3.27–3.00 (m, 2H), 1.90–1.75 (m, 2H), 1.42–1.22 (m, 8H), 0.85 (t, J = 6.9 Hz, 3H). ^{13}C NMR (100 MHz, CDCl_3) δ 159.10

(2 × C), 155.45, 149.03 (2 × CH), 141.98, 139.69, 136.79 (2 × CH), 126.40, 124.60, 123.28 (2 × CH), 123.16, 122.28 (2 × CH), 122.21, 119.00, 111.99, 108.12, 101.88, 100.61, 70.12, 68.06, 60.53, 58.53, 50.83, 43.31, 31.81, 29.17, 29.09, 27.32, 22.68, 14.16. HRMS (ESI+): calculated for C₃₄H₄₁N₄O₂ [M + H]⁺ 537.3230, found 537.3220. HPLC purity: 98.4%, t_R = 9.0 min.

1-(Bis(pyridin-2-ylmethyl)amino)-3-((9-nonyl-9H-carbazol-4-yl)-oxy)propan-2-ol (14). 14 was synthesized from 2,2'-dipicolylamine (0.2 mL) and 6 (32.8 mg, 0.09 mmol) according to the similar procedure for 9 to give 14 as a dark green solid (33.6 mg, 66%); mp 66.1–67.5 °C. ¹H NMR (400 MHz, CDCl₃) δ 8.59–8.49 (m, 2H), 8.14 (d, J = 7.7 Hz, 1H), 7.63–7.47 (m, 2H), 7.46–7.29 (m, 5H), 7.18–6.98 (m, 4H), 6.65 (d, J = 7.9 Hz, 1H), 4.46–4.37 (m, 3H), 4.33–4.17 (m, 4H), 4.11–3.98 (m, 3H), 3.28–2.99 (m, 2H), 1.91–1.76 (m, 2H), 1.41–1.21 (m, 12H), 0.86 (t, J = 6.9 Hz, 3H). ¹³C NMR (100 MHz, CDCl₃) δ 159.08 (2 × C), 155.45, 149.04 (2 × CH), 141.98, 139.70, 136.79 (2 × CH), 126.41, 124.60, 123.29 (2 × CH), 123.16, 122.28 (2 × CH), 122.21, 119.01, 111.99, 108.13, 101.89, 100.62, 70.13, 68.05, 60.54 (2 × CH₂), 58.52, 43.30, 31.91, 29.56, 29.51, 29.34, 29.07, 27.35, 22.73, 14.21. HRMS (ESI+): calculated for C₃₆H₄₅N₄O₂ [M + H]⁺ 565.3543, found 565.3535. HPLC purity: 99.1%, t_R = 5.6 min.

1-(Bis(pyridin-2-ylmethyl)amino)-3-((9-(4,4,4-trifluorobutyl)-9H-carbazol-4-yl)oxy)propan-2-ol (15). 15 was synthesized from 2,2'-dipicolylamine (0.2 mL) and 7 (56.3 mg, 0.16 mmol) according to the similar procedure for 9. The product 15 was obtained as a dark green solid (53.2 mg, 60%); mp 62.1–63.9 °C. ¹H NMR (400 MHz, CDCl₃) δ 8.30 (d, J = 4.2 Hz, 2H), 8.00 (d, J = 7.7 Hz, 1H), 7.55–7.45 (m, 4H), 7.44–7.31 (m, 3H), 7.11–7.00 (m, 4H), 6.66 (d, J = 8.0 Hz, 1H), 4.45–4.26 (m, 3H), 4.21 (d, J = 3.9 Hz, 2H), 3.98–3.85 (m, 4H), 3.14–2.88 (m, 2H), 2.23–2.02 (m, 4H). ¹³C NMR (100 MHz, CDCl₃) δ 159.54, 156.62, 149.21 (2 × CH), 142.97, 140.70, 138.75, 129.97, 127.82 (2 × CH), 127.23, 125.86, 125.00 (2 × CH), 124.31, 123.78 (2 × CH), 123.43, 120.29, 113.24, 109.05, 102.81, 101.96, 70.59, 68.97, 61.58, 58.50, 42.37, 32.11, 31.82, 22.74. HRMS (ESI+): calculated for C₃₁H₃₂F₃N₄O₂ [M + H]⁺ 549.2477, found 549.2465. HPLC purity: 99.4%, t_R = 5.7 min.

1-(Bis(pyridin-2-ylmethyl)amino)-3-((9-(3-methylbut-2-en-1-yl)-9H-carbazol-4-yl)oxy)propan-2-ol (16). 16 was prepared from 2,2'-dipicolylamine (0.2 mL) and 8 (100 mg, 0.33 mmol) according to the similar procedure for 9 to give 16 as a dark green solid (106.9 mg, 74%); mp 56.1–57.8 °C. ¹H NMR (400 MHz, CDCl₃) δ 8.58–8.54 (m, 2H), 8.16 (d, J = 7.8 Hz, 1H), 7.61–7.54 (m, 2H), 7.42–7.31 (m, 5H), 7.16–7.07 (m, 3H), 6.99 (d, J = 8.1 Hz, 1H), 6.65 (d, J = 8.0 Hz, 1H), 5.28–5.22 (m, 1H), 4.86 (d, J = 6.4 Hz, 2H), 4.43–4.35 (m, 1H), 4.34–4.16 (m, 2H), 4.13–3.96 (m, 4H), 3.27–2.98 (m, 2H), 1.94–1.89 (m, 3H), 1.71–1.67 (m, 3H). ¹³C NMR (100 MHz, CDCl₃) δ 158.91 (2 × C), 155.43, 148.86 (2 × CH), 141.85, 139.57, 136.93 (2 × CH), 135.08, 126.41 (2 × C), 124.62, 123.38 (2 × CH), 123.16, 122.35 (2 × CH), 120.09, 119.10, 112.17, 108.21, 101.97, 100.79, 70.13, 68.03, 60.44, 58.54, 41.35, 25.65, 18.28. HRMS (ESI+): calculated for C₃₂H₃₅N₄O₂ [M + H]⁺ 507.2760, found 507.2761. HPLC purity: 99.2%, t_R = 6.6 min.

1-((9-(3-Methylbut-2-en-1-yl)-9H-carbazol-4-yl)oxy)-3-((pyridin-2-ylmethyl)amino)propan-2-ol (19). 19 was prepared from 2-picolylamine (0.2 mL) and 8 (50 mg, 0.16 mmol) according to the similar procedure for 9 to provide 19 as a dark green solid (48.6 mg, 72%); mp 74.5–76.4 °C. ¹H NMR (400 MHz, DMSO-d₆) δ 8.46–8.38 (m, 1H), 8.16–8.03 (m, 1H), 7.67–7.45 (m, 1H), 7.38–7.28 (m, 2H), 7.28–7.20 (m, 2H), 7.15–7.00 (m, 2H), 6.95–6.87 (m, 1H), 6.62–6.48 (m, 1H), 5.22–5.09 (m, 1H), 4.87–4.66 (m, 4H), 4.56–4.02 (m, 5H), 3.81–3.63 (m, 1H), 3.29–2.99 (m, 1H), 1.88–1.75 (m, 3H), 1.68–1.55 (m, 3H). ¹³C NMR (100 MHz, CD₃OD) δ 156.21, 154.93, 150.29, 143.08, 140.83, 138.67, 136.26, 127.51, 125.76, 124.50, 124.16, 124.00, 123.29, 121.06, 120.04, 113.13, 109.48, 103.51, 101.86, 70.96, 67.84, 52.87, 51.92, 41.90, 25.73, 18.21. HRMS (ESI+): calculated for C₂₆H₃₀N₃O₂ [M + H]⁺ 416.2338, found 416.2330. HPLC purity: 99.3%, t_R = 5.8 min.

MIC Determinations. The MIC values were determined as described in previous reports with minor modifications.⁴³ Test

compounds were dissolved in DMSO/H₂O to prepare a 1000 μg/mL stock solution. Then, the stock solution was diluted with Muller Hinton broth (MHB) containing ZnSO₄·H₂O (final Zn²⁺ concentration of 0, 6.25, or 12.5 μg/mL). The bacteria were inoculated on the Mueller Hinton agar (MHA) plate at 37 °C overnight and adjusted to approximately 10⁶ CFU/mL. Bacterial suspensions (100 μL) were mixed with 100 μL two-fold serial dilutions of test compounds (final compound concentrations of 50, 25, 12.5, 6.25, 3.125, 1.56, 0.78, and 0.39 μg/mL) in a 96-well plate. The plate was incubated for 24 h at 37 °C. Then, a Biotek multi-detector microplate reader was used to read the absorption wavelength of the mixture at 600 nm. MICs were determined as the lowest compound concentration, which inhibited 95% of the bacterial growth. The experiments were performed at least twice with biologically replicates.

Hemolytic Assay. The hemolysis experiment was carried out as described in our previous reports.⁴³ Briefly, compounds were dissolved in DMSO to prepare 40 mg/mL stock solutions and two-fold serially diluted with PBS (final concentration of DMSO = 0.5%) in 96-well plates. Then, rabbit red blood cells (RBCs) were centrifuged at 2500 rpm for 3 min, washed twice with PBS, and suspended in PBS to make an 8% v/v RBCs suspension. The RBCs suspension was mixed with an equal volume of two-fold serial dilutions of compounds in 96-well plates and incubated at 37 °C for 1 h. The 96-well plate was centrifuged at 2500 rpm for 5 min. Then, the supernatant (100 μL) was transferred into another 96-well plate. A Biotek multi-detector microplate reader was used to read the absorption wavelength of the mixture at 576 nm. A 2% Triton X-100 solution treatment was used as a positive control, and 0.5% DMSO treatment was used as a negative control. Hemolytic activity was calculated by the following formula: % hemolysis = [(Abs_{sample} – Abs_{negative control})/(Abs_{positive control} – Abs_{negative control})] × 100. The experiments were performed at least twice with three duplicates for each time.

Time-Kill Study. The time-kill experiment was performed as described in previous reports with minor modifications.⁴³ The *in vitro* time-kill kinetics of compound 16 in the presence of 12.5 μg/mL Zn²⁺ were performed against *S. aureus* ATCC29213 and *E. coli* ATCC25922. The bacteria were adjusted to approximately 10⁶ CFU/mL. The bacterial suspension was incubated with compound 16 at different concentrations (4× and 8× MIC) in the presence of 12.5 μg/mL Zn²⁺ at 37 °C. Aliquots were then removed from the mixture at different time points (0.5, 1, 2, 4, 8, and 24 h), 10-fold serially diluted in PBS, and plated onto MHA plates. The plates were incubated for 24 h at 37 °C, and the bacterial colonies grown on the plates were counted. The experiments were carried out at least twice.

Drug Resistance Study. The drug resistance experiment was performed as described in previous reports with minor modifications.⁴³ According to the above-mentioned methods, the initial MICs of the compounds against *S. aureus* ATCC29213 and *E. coli* ATCC25922 were obtained. The bacteria from the wells at 0.5× MIC concentration of compounds were then used to prepare the bacterial suspension for the next MIC value test. The experiment was repeated every day for 19 days.

SYTOX Green Assay. This experiment was performed as described in previous reports with minor modifications.⁴³ *S. aureus* ATCC29213 or *E. coli* ATCC 25922 was incubated in MHB at 37 °C overnight and centrifuged at 5000 rpm for 5 min. Then, the supernatant was removed. The inoculum was washed three times with PBS (pH = 7.2) and resuspended in PBS to prepare bacterial suspension (OD₆₀₀ = 0.2). SYTOX Green dye (0.3 μM) was added to the bacterial suspension and cultured in the dark. The fluorescence intensity of mixture was monitored by a Biotek multi-detector microplate reader (emission and excitation wavelengths were 523 and 504 nm, respectively). After the fluorescence signal was stabilized, different concentrations (2×, 4×, and 8× MIC) of compound 16 in the presence of 12.5 μg/mL Zn²⁺ were added to the mixture, and the fluorescence intensity change was monitored and recorded for about 1 h. The experiments were carried out at least twice with biologically replicates.

DiSC₃ (5) Assay. This experiment was performed as described in previous reports with minor modifications.⁶⁸ DiSC₃ (5) was used to measure the depolarization of the bacterial cell membranes of *S. aureus* ATCC29213 or *E. coli* ATCC 25922 after the treatment of compound **16** combined with 12.5 $\mu\text{g/mL}$ Zn^{2+} . The bacteria (*S. aureus* ATCC29213 or *E. coli* ATCC 25922) were incubated in MHB at 37 °C overnight and were centrifuged at 5000 rpm for 5 min. Then, the supernatant was removed. The inoculum was washed three times with HEPES (5 mM, pH = 7.2) and resuspended in HEPES to prepare bacterial suspension (OD₆₀₀ = 0.3). DiSC₃ (5) dye (0.2 μM) was added to the bacterial suspension. The mixture was incubated for 15 min in the dark. A Biotek multi-detector microplate reader (emission and excitation wavelengths were 670 and 622 nm, respectively) was used to monitor the fluorescence intensity of the mixture. After the fluorescence signal was stabilized, different concentrations (2 \times , 4 \times , and 8 \times MIC) of compound **16** in the presence of 12.5 $\mu\text{g/mL}$ Zn^{2+} were added to the mixture, and the fluorescence intensity change was monitored and recorded for about 1 h. The experiments were carried out at least twice with biologically replicates.

1-N-Phenyl-naphthylamine Uptake Assay. This experiment was performed as described in previous reports with minor modifications.⁶⁹ NPN uptake assay was used to determine the permeability of the outer membranes of *E. coli* ATCC25922. The bacteria (*E. coli* ATCC25922) were incubated in MHB at 37 °C overnight and were centrifuged at 5000 rpm for 5 min. Then, the supernatant was removed. The inoculum was washed three times with HEPES (5 mM, pH = 7.2) and resuspended in HEPES to prepare the bacterial suspension with a cell density of approximately 1×10^8 CFU/mL. NPN (10 μM) was added to the bacterial suspension. The fluorescence intensity of the mixture was monitored by a Biotek multi-detector microplate reader (emission and excitation wavelengths were 420 and 350 nm, respectively). After the fluorescence signal was stabilized, different concentrations (1 \times , 2 \times , 4 \times , and 8 \times MIC) of compound **16** in the presence of 12.5 $\mu\text{g/mL}$ Zn^{2+} were added to the mixture, and the fluorescence intensity change was monitored and recorded for about 1 h. The experiments were carried out at least twice with biologically replicates.

LIVE/DEAD Fluorescence Staining Assay. This experiment was performed as described in previous reports with minor modifications.⁴³ LIVE/DEAD BacLight bacterial viability kit L7007 (ThermoFisher, USA) was used to determine the membrane integrity of bacterial cells. The bacteria (*S. aureus* ATCC29213 or *E. coli* ATCC 25922) were incubated in MHB to the logarithmic growth phase and were centrifuged at 5000 rpm for 5 min. Then, the supernatant was removed. The bacterial cells were washed twice with PBS (10 mM, pH = 7.2) and resuspended in PBS to prepare the bacterial suspension with a cell density of approximately 1×10^8 CFU/mL. The bacterial suspension was mixed with compound **16** in the presence of 12.5 $\mu\text{g/mL}$ Zn^{2+} (final concentration of 8 \times MIC) or PBS (negative control) and incubated for 2 h at 37 °C. Then, these bacterial cells were stained with SYTO 9 (5 μM) and PI (30 μM) for 15 min in the dark. Finally, the bacterial cells were prepared into smears and were observed under a laser confocal microscope (ZEISS LSM 880). The experiments were carried out at least twice with biologically replicates.

BODIPY-TR-Cadaverine Displacement Assay. This experiment was performed as described in previous reports with minor modifications.^{65,70} Binding affinity between compound **16** combined with 12.5 $\mu\text{g/mL}$ Zn^{2+} and lipopolysaccharides (LPS) was investigated by using BODIPY-TR-cadaverine displacement assay. BODIPY-TR-cadaverine and LPS from *P. aeruginosa* were obtained from ThermoFisher and Sigma-Aldrich, respectively. BODIPY-TR-cadaverine (final concentration of 5 μM) and LPS (final concentration of 12.5 $\mu\text{g/mL}$) were prepared using Tris buffer (50 mM, pH 7.4) in 24-well plates. After 15 min, compound **16** (1 \times , 2 \times , 4 \times , 8 \times , and 16 \times MIC) in the presence of 12.5 $\mu\text{g/mL}$ Zn^{2+} or without Zn^{2+} was added. The plates were kept in the dark at room temperature for 30 min. Finally, fluorescence intensity was recorded by a Biotek multi-detector microplate reader, using excitation and

emission wavelength of 580 and 620 nm, respectively. The experiments were carried out at least twice with biologically replicates.

CCK-8 Assay. This experiment was performed as described in previous reports with minor modifications.⁴³ The cytotoxicity of compound **16** in the presence of 12.5 $\mu\text{g/mL}$ Zn^{2+} toward mouse fibroblasts (NCTC clone 929) was determined using CCK-8 assay according to a previously reported method. Compound **16** in the presence of 12.5 $\mu\text{g/mL}$ Zn^{2+} was incubated with mouse fibroblasts for 24 h. All measurements were carried out at least twice with biological replicates.

In Vivo Efficacy. The animal studies were performed as described in previous reports with minor modifications.⁴³ All animal experiments were approved by the Laboratory Animal Center of South China Agricultural University and performed in accordance with the policy of the Ministry of Health. Six to 8 week-old female C57BL6 mice (approximately 20 g weight) purchased from Vital River Laboratory Animal Technology Co., Ltd. were used in this study. The bacteria (*S. aureus* ATCC29213 or *P. aeruginosa* ATCC9027) were grown on MHA plates at 37 °C for 24 h, and the cell concentration of the bacterial suspension was adjusted with PBS to approximately 5×10^7 CFU/mL for mice corneal infection.

The murine corneal infection model induced by *S. aureus* ATCC29213 were immunosuppressed using cyclophosphamide (100 mg/kg) via intraperitoneal injection three times 5 days before infection. In the murine corneal infection model induced by *P. aeruginosa* ATCC9027, the mice did not be immunosuppressed. The mice were anesthetized by intraperitoneal injection of 2.5% avertin solution (500 mg/kg), and the right corneal scratches were created by sterile needles. Fifteen microliters of the bacterial inoculum (*S. aureus* ATCC29213 or *P. aeruginosa* ATCC9027) was dripped onto the injured cornea. All mice were randomly divided into 6 groups, five mice per group ($n = 5$), 3 groups of mice were used in the *S. aureus* ATCC29213-induced murine corneal infection study, and the other 3 groups of mice were used in the *P. aeruginosa* ATCC9027-induced murine corneal infection study. One day after infection, the corresponding drugs (0.5% compound **16** containing 12.5 $\mu\text{g/mL}$ Zn^{2+} , 5% vancomycin as the positive control toward *S. aureus* ATCC29213, and 0.3% gatifloxacin as the positive control toward *P. aeruginosa* ATCC9027) were given topically four times every day for 3 days. Finally, all mice were sacrificed, and the wounded corneas were removed. The number of living bacteria on the cornea was counted by a standard plate counting method using MHA plates. Statistical significance was calculated by the SPSS 22.0 software. *P* values were calculated by the independent *t* test, and $P < 0.05$ was considered to be significant.

■ ASSOCIATED CONTENT

Supporting Information

The Supporting Information is available free of charge at <https://pubs.acs.org/doi/10.1021/acs.jmedchem.1c00858>.

In vitro salt resistance study; mass analysis of complex formation of compound **16** with Zn^{2+} ; Table S1; Figure S1; Figure S2; NMR spectra, HR-MS spectra, and HPLC traces of synthesized carbazole derivatives (PDF) Molecular formula strings (CSV)

■ AUTHOR INFORMATION

Corresponding Authors

Shouping Liu – Key Laboratory of Molecular Target & Clinical Pharmacology and the State Key Laboratory of Respiratory Disease, School of Pharmaceutical Sciences & the Fifth Affiliated Hospital, Guangzhou Medical University, Guangzhou 511436, P.R. China; Email: liushouping2018@163.com

Shuimu Lin – Key Laboratory of Molecular Target & Clinical Pharmacology and the State Key Laboratory of Respiratory Disease, School of Pharmaceutical Sciences & the Fifth

Affiliated Hospital, Guangzhou Medical University, Guangzhou 511436, P.R. China; orcid.org/0000-0002-0477-8173; Email: linshuimu020@163.com

Authors

Jiayong Liu – Key Laboratory of Molecular Target & Clinical Pharmacology and the State Key Laboratory of Respiratory Disease, School of Pharmaceutical Sciences & the Fifth Affiliated Hospital, Guangzhou Medical University, Guangzhou 511436, P.R. China; orcid.org/0000-0002-1834-0877

Hongxia Li – Key Laboratory of Molecular Target & Clinical Pharmacology and the State Key Laboratory of Respiratory Disease, School of Pharmaceutical Sciences & the Fifth Affiliated Hospital, Guangzhou Medical University, Guangzhou 511436, P.R. China

Haizhou Li – Key Laboratory of Molecular Target & Clinical Pharmacology and the State Key Laboratory of Respiratory Disease, School of Pharmaceutical Sciences & the Fifth Affiliated Hospital, Guangzhou Medical University, Guangzhou 511436, P.R. China

Shanfang Fang – Key Laboratory of Molecular Target & Clinical Pharmacology and the State Key Laboratory of Respiratory Disease, School of Pharmaceutical Sciences & the Fifth Affiliated Hospital, Guangzhou Medical University, Guangzhou 511436, P.R. China

Jinguo Shi – Department of Medicinal Chemistry, School of Pharmaceutical Science, Sun Yat-sen University, Guangzhou 510006, P. R. China

Yongzhi Chen – Key Laboratory of Molecular Target & Clinical Pharmacology and the State Key Laboratory of Respiratory Disease, School of Pharmaceutical Sciences & the Fifth Affiliated Hospital, Guangzhou Medical University, Guangzhou 511436, P.R. China

Rongcui Zhong – Key Laboratory of Molecular Target & Clinical Pharmacology and the State Key Laboratory of Respiratory Disease, School of Pharmaceutical Sciences & the Fifth Affiliated Hospital, Guangzhou Medical University, Guangzhou 511436, P.R. China

Complete contact information is available at:

<https://pubs.acs.org/10.1021/acs.jmedchem.1c00858>

Author Contributions

#J.L. and H.X.L. contributed equally. S.M.L. and S.P.L. designed and coordinated the whole study. The experiments were carried out by J.L., H.X.L., H.Z.L., S.F., J.S., Y.C., and R.Z.; J.L., H.X.L., and S.M.L. analyzed the data. The manuscript was written with contributions from all authors. All authors have approved the final version of the manuscript.

Funding

This work was supported by the National Natural Science Foundation of China (21907019 to S.M.L.) and the Talent Fund for High-Level University Construction of Guangzhou (B195002009029 to S.P.L. and B195002009030 to S.M.L.).

Notes

The authors declare no competing financial interest.

ABBREVIATIONS

LPS, lipopolysaccharide; CAMPs, cationic antimicrobial peptides; DPA, dipicolylamine; LTA, lipoteichoic acid; PI, propidium iodide; MRSA, methicillin-resistant *S. aureus*; PBS, phosphate-buffered saline; RBCs, red blood cells; NPN, 1-N-

phenylmethylamine; MIC, minimum inhibitory concentration; MHB, Mueller Hinton broth; CFU, colony-forming units; VAN, vancomycin; CIP, ciprofloxacin; NMR, nuclear magnetic resonance; HPLC, high-performance liquid chromatography; HRMS, high-resolution mass spectrometry; NCTC, National Collection of Type Cultures; ATCC, American Type Culture Collection

REFERENCES

- (1) Harris, S. R.; Feil, E. J.; Holden, M. T. G.; Quail, M. A.; Nickerson, E. K.; Chantratita, N.; Gardete, S.; Tavares, A.; Day, N.; Lindsay, J. A.; Edgeworth, J. D.; de Lencastre, H.; Parkhill, J.; Peacock, S. J.; Bentley, S. D. Evolution of MRSA during hospital transmission and intercontinental spread. *Science* **2010**, *327*, 469–474.
- (2) O'Connell, K. M. G.; Hodgkinson, J. T.; Sore, H. F.; Welch, M.; Salmond, G. P. C.; Spring, D. R. Combating multidrug-resistant bacteria: current strategies for the discovery of novel antibacterials. *Angew. Chem., Int. Ed.* **2013**, *52*, 10706–10733.
- (3) Wilyard, C. The drug-resistant bacteria that pose the greatest health threats. *Nature* **2017**, *543*, 15.
- (4) Goff, D. A.; Kullar, R.; Goldstein, E. J. C.; Gilchrist, M.; Nathwani, D.; Cheng, A. C.; Cairns, K. A.; Escandón-Vargas, K.; Villegas, M. V.; Brink, A.; van den Bergh, D.; Mendelson, M. A global call from five countries to collaborate in antibiotic stewardship: united we succeed, divided we might fail. *Lancet Infect. Dis.* **2017**, *17*, e56–e63.
- (5) Luong, H. X.; Thanh, T. T.; Tran, T. H. Antimicrobial peptides - Advances in development of therapeutic applications. *Life Sci.* **2020**, *260*, 118407–118407.
- (6) Ashiru-Oredope, D.; Hopkins, S. Antimicrobial resistance: moving from professional engagement to public action. *J. Antimicrob. Chemother.* **2015**, *70*, 2927–2930.
- (7) Silver, L. L. Challenges of antibacterial discovery. *Clin. Microbiol. Rev.* **2011**, *24*, 71–109.
- (8) Butler, M. S.; Blaskovich, M. A. T.; Cooper, M. A. Antibiotics in the clinical pipeline at the end of 2015. *J. Antibiot.* **2017**, *70*, 3–24.
- (9) Richter, M. F.; Drown, B. S.; Riley, A. P.; Garcia, A.; Shirai, T.; Svec, R. L.; Hergenrother, P. J. Predictive compound accumulation rules yield a broad-spectrum antibiotic. *Nature* **2017**, *545*, 299–304.
- (10) Boll, J. M.; Crofts, A. A.; Peters, K.; Cattoir, V.; Vollmer, W.; Davies, B. W.; Trent, M. S. A penicillin-binding protein inhibits selection of colistin-resistant, lipooligosaccharide-deficient *Acinetobacter baumannii*. *Proc. Natl. Acad. Sci. U. S. A.* **2016**, *113*, E6228–e6237.
- (11) Tacconelli, E.; Carrara, E.; Savoldi, A.; Harbarth, S.; Mendelson, M.; Monnet, D. L.; Pulcini, C.; Kahlmeter, G.; Kluytmans, J.; Carmeli, Y.; Ouellette, M.; Outtersson, K.; Patel, J.; Cavaleri, M.; Cox, E. M.; Houchens, C. R.; Grayson, M. L.; Hansen, P.; Singh, N.; Theuretzbacher, U.; Magrini, N. Discovery, research, and development of new antibiotics: the WHO priority list of antibiotic-resistant bacteria and tuberculosis. *Lancet Infect. Dis.* **2018**, *18*, 318–327.
- (12) Martin, J. K., II; Sheehan, J. P.; Bratton, B. P.; Moore, G. M.; Mateus, A.; Li, S. H.-J.; Kim, H.; Rabinowitz, J. D.; Typas, A.; Savitski, M. M.; Wilson, M. Z.; Gitai, Z. A dual-mechanism antibiotic kills Gram-negative bacteria and avoids drug resistance. *Cell* **2020**, *181*, 1518–1532.e14.
- (13) Lee, S. H.; Jun, H. K.; Lee, H. R.; Chung, C. P.; Choi, B. K. Antibacterial and lipopolysaccharide (LPS)-neutralising activity of human cationic antimicrobial peptides against periodontopathogens. *Int. J. Antimicrob. Agents* **2010**, *35*, 138–145.
- (14) Mookherjee, N.; Anderson, M. A.; Haagsman, H. P.; Davidson, D. J. Antimicrobial host defence peptides: functions and clinical potential. *Nat. Rev. Drug Discovery* **2020**, *19*, 311–332.
- (15) Torrent, M.; Pulido, D.; Rivas, L.; Andreu, D. Antimicrobial peptide action on parasites. *Curr. Drug Targets* **2012**, *13*, 1138–1147.
- (16) Bechinger, B.; Gorr, S. U. Antimicrobial peptides: mechanisms of action and resistance. *J. Dent. Res.* **2016**, *96*, 254–260.

- (17) Etayash, H.; Pletzer, D.; Kumar, P.; Straus, S. K.; Hancock, R. E. W. Cyclic derivative of host-defense peptide IDR-1018 improves proteolytic stability, suppresses inflammation, and enhances in vivo activity. *J. Med. Chem.* **2020**, *63*, 9228–9236.
- (18) Sani, M. A.; Separovic, F. How membrane-active peptides get into lipid membranes. *Acc. Chem. Res.* **2016**, *49*, 1130–1138.
- (19) Guha, S.; Ghimire, J.; Wu, E.; Wimley, W. C. Mechanistic landscape of membrane-permeabilizing peptides. *Chem. Rev.* **2019**, *119*, 6040–6085.
- (20) Shukla, R.; Medeiros-Silva, J.; Parmar, A.; Vermeulen, B. J. A.; Das, S.; Paioni, A. L.; Jekhmane, S.; Lorent, J.; Bonvin, A. M. J. J.; Baldus, M.; Lelli, M.; Veldhuizen, E. J. A.; Breukink, E.; Singh, I.; Weingarth, M. Mode of action of teixobactins in cellular membranes. *Nat. Commun.* **2020**, *11*, 2848.
- (21) Mojsoska, B.; Zuckermann, R. N.; Jossen, H. Structure-activity relationship study of novel peptoids that mimic the structure of antimicrobial peptides. *Antimicrob. Agents Chemother.* **2015**, *59*, 4112–4120.
- (22) Kintsès, B.; Jangir, P. K.; Fekete, G.; Számel, M.; Méhi, O.; Spohn, R.; Daruka, L.; Martins, A.; Hosseinnia, A.; Gagarinova, A.; Kim, S.; Phanse, S.; Csörgő, B.; Györkei, Á.; Ari, E.; Lázár, V.; Nagy, I.; Babu, M.; Pál, C.; Papp, B. Chemical-genetic profiling reveals limited cross-resistance between antimicrobial peptides with different modes of action. *Nat. Commun.* **2019**, *10*, 5731.
- (23) Scott, R. W.; Tew, G. N. Mimics of host defense proteins; strategies for translation to therapeutic applications. *Curr. Top. Med. Chem.* **2017**, *17*, 576–589.
- (24) Luther, A.; Urfer, M.; Zahn, M.; Müller, M.; Wang, S.-Y.; Mondal, M.; Vitale, A.; Hartmann, J.-B.; Sharpe, T.; Monte, F. L.; Kocherla, H.; Cline, E.; Pessi, G.; Rath, P.; Modaresi, S. M.; Chiquet, P.; Stiegeler, S.; Verbree, C.; Remus, T.; Schmitt, M.; Kolopp, C.; Westwood, M.-A.; Desjonquères, N.; Brabet, E.; Hell, S.; LePoupon, K.; Vermeulen, A.; Jaisson, R.; Rithié, V.; Upert, G.; Lederer, A.; Zbinden, P.; Wach, A.; Moehle, K.; Zerbe, K.; Locher, H. H.; Bernardini, F.; Dale, G. E.; Eberl, L.; Wollscheid, B.; Hiller, S.; Robinson, J. A.; Obrecht, D. Chimeric peptidomimetic antibiotics against Gram-negative bacteria. *Nature* **2019**, *576*, 452–458.
- (25) Sgolastra, F.; Deronde, B. M.; Sarapas, J. M.; Som, A.; Tew, G. N. Designing mimics of membrane active proteins. *Acc. Chem. Res.* **2013**, *46*, 2977–2987.
- (26) Lin, S.; Koh, J. J.; Aung, T. T.; Sin, W. L. W.; Lim, F.; Wang, L.; Lakshminarayanan, R.; Zhou, L.; Tan, D. T. H.; Cao, D.; Beuerman, R. W.; Ren, L.; Liu, S. Semisynthetic flavone-derived antimicrobials with therapeutic potential against methicillin-resistant *Staphylococcus aureus* (MRSA). *J. Med. Chem.* **2017**, *60*, 6152–6165.
- (27) Lin, S.; Sin, W. L. W.; Koh, J. J.; Lim, F.; Wang, L.; Cao, D.; Beuerman, R. W.; Ren, L.; Liu, S. Semisynthesis and biological evaluation of xanthone amphiphilics as selective, highly potent antifungal agents to combat fungal resistance. *J. Med. Chem.* **2017**, *60*, 10135–10150.
- (28) Lin, S.; Koh, J.-J.; Aung, T. T.; Lim, F.; Li, J.; Zou, H.; Wang, L.; Lakshminarayanan, R.; Verma, C.; Wang, Y.; Tan, D. T. H.; Cao, D.; Beuerman, R. W.; Ren, L.; Liu, S. Symmetrically substituted xanthone amphiphiles combat Gram-positive bacterial resistance with enhanced membrane selectivity. *J. Med. Chem.* **2017**, *60*, 1362–1378.
- (29) Koh, J. J.; Lin, S.; Aung, T. T.; Lim, F.; Zou, H.; Bai, Y.; Li, J.; Lin, H.; Pang, L. M.; Koh, W. L.; Salleh, S. M.; Lakshminarayanan, R.; Zhou, L.; Qiu, S.; Pervushin, K.; Verma, C.; Tan, D. T.; Cao, D.; Liu, S.; Beuerman, R. W. Amino acid modified xanthone derivatives: novel, highly promising membrane-active antimicrobials for multidrug-resistant Gram-positive bacterial infections. *J. Med. Chem.* **2015**, *58*, 739–752.
- (30) Bera, S.; Zhanel, G. G.; Schweizer, F. Evaluation of amphiphilic aminoglycoside-peptide triazole conjugates as antibacterial agents. *Bioorg. Med. Chem. Lett.* **2010**, *20*, 3031–3035.
- (31) Zimmermann, L.; Das, I.; Désiré, J.; Sautrey, G.; Barros, R. S. V.; El Khoury, M.; Mingeot-Leclercq, M.-P.; Décout, J.-L. New broad-spectrum antibacterial amphiphilic aminoglycosides active against resistant bacteria: from neamine derivatives to smaller neosamine analogues. *J. Med. Chem.* **2016**, *59*, 9350–9369.
- (32) Isaksson, J.; Brandsdal, B. O.; Engqvist, M.; Flaten, G. E.; Mjøen Svendsen, J. S.; Stensen, W. A synthetic antimicrobial peptidomimetic (LTX 109): stereochemical impact on membrane disruption. *J. Med. Chem.* **2011**, *54*, 5786–5795.
- (33) Kowalski, R. P.; Romanowski, E. G.; Yates, K. A.; Mah, F. S. An independent evaluation of a novel peptide mimetic, Brilacidin (PMX30063), for ocular anti-infective. *J. Ocul. Pharmacol. Ther.* **2016**, *32*, 23–27.
- (34) Rouéssé, J.; Spielmann, M.; Turpin, F.; Le Chevalier, T.; Azab, M.; Mondésir, J. M. Phase II study of elliptinium acetate salvage treatment of advanced breast cancer. *Eur. J. Cancer* **1993**, *29*, 856–859.
- (35) Stiborová, M.; Frei, E.; Schmeiser, H. H.; Arlt, V. M.; Martínek, V. Mechanisms of enzyme-catalyzed reduction of two carcinogenic nitro-aromatics, 3-nitrobenzanthrone and aristolochic acid I: Experimental and theoretical approaches. *Int. J. Mol. Sci.* **2014**, *15*, 10271–10295.
- (36) Ramirez-Soto, I.; Rodriguez, E.; Alvarez, R.; Quiroz, E.; Ortega, A. Intracellular effect of β 3-adrenoceptor agonist Carazolol on skeletal muscle, a direct interaction with SERCA. *Cell Calcium* **2019**, *79*, 20–26.
- (37) Avila, M. S.; Ayub-Ferreira, S. M.; de Barros Wanderley, M. R.; das Dores Cruz, F.; Gonçalves Brandão, S. M.; Rigaud, V. O. C.; Higuchi-Dos-Santos, M. H.; Hajjar, L. A.; Kalil Filho, R.; Hoff, P. M.; Sahade, M.; Ferrari, M. S. M.; de Paula Costa, R. L.; Mano, M. S.; Bittencourt Viana Cruz, C. B.; Abduch, M. C.; Lofrano Alves, M. S.; Guimaraes, G. V.; Issa, V. S.; Bittencourt, M. S.; Bocchi, E. A. Carvedilol for prevention of chemotherapy-related cardiotoxicity: the CECCY trial. *J. Am. Coll. Cardiol.* **2018**, *71*, 2281–2290.
- (38) Bandgar, B. P.; Adsul, L. K.; Chavan, H. V.; Jalde, S. S.; Shringare, S. N.; Shaikh, R.; Meshram, R. J.; Gacche, R. N.; Masand, V. Synthesis, biological evaluation, and docking studies of 3-(substituted)-aryl-5-(9-methyl-3-carbazole)-1H-2-pyrazolines as potent anti-inflammatory and antioxidant agents. *Bioorg. Med. Chem. Lett.* **2012**, *22*, 5839–5844.
- (39) Gu, W.; Wang, S. Synthesis and antimicrobial activities of novel 1H-dibenzo[a,c]carbazoles from dehydroabiatic acid. *Eur. J. Med. Chem.* **2010**, *45*, 4692–4696.
- (40) Thevissen, K.; Marchand, A.; Chaltin, P.; Meert, E.; Cammue, B. Antifungal carbazoles. *Curr. Med. Chem.* **2009**, *16*, 2205–2211.
- (41) Maji, B.; Kumar, K.; Kaulage, M.; Muniyappa, K.; Bhattacharya, S. Design and synthesis of new benzimidazole-carbazole conjugates for the stabilization of human telomeric DNA, telomerase inhibition, and their selective action on cancer cells. *J. Med. Chem.* **2014**, *57*, 6973–6988.
- (42) Tachibana, Y.; Kikuzaki, H.; Lajis, N. H.; Nakatani, N. Antioxidative activity of carbazoles from *Murraya koenigii* leaves. *J. Agric. Food Chem.* **2001**, *49*, 5589–5594.
- (43) Lin, S.; Liu, J.; Li, H.; Liu, Y.; Chen, Y.; Luo, J.; Liu, S. Development of highly potent carbazole amphiphiles as membrane-targeting antimicrobials for treating Gram-positive bacterial infections. *J. Med. Chem.* **2020**, *63*, 9284–9299.
- (44) Jeżowska-Bojczuk, M.; Stokowa-Soltys, K. Peptides having antimicrobial activity and their complexes with transition metal ions. *Eur. J. Med. Chem.* **2018**, *143*, 997–1009.
- (45) Silverman, J. A.; Perlmutter, N. G.; Shapiro, H. M. Correlation of daptomycin bactericidal activity and membrane depolarization in *Staphylococcus aureus*. *Antimicrob. Agents Chemother.* **2003**, *47*, 2538–2544.
- (46) Karas, J. A.; Carter, G. P.; Howden, B. P.; Turner, A. M.; Paulin, O. K. A.; Swarbrick, J. D.; Baker, M. A.; Li, J.; Velkov, T. Structure-activity relationships of Daptomycin lipopeptides. *J. Med. Chem.* **2020**, *63*, 13266–13290.
- (47) Grein, F.; Müller, A.; Scherer, K. M.; Liu, X.; Ludwig, K. C.; Klöckner, A.; Strach, M.; Sahl, H. G.; Kubitscheck, U.; Schneider, T. Ca²⁺-Daptomycin targets cell wall biosynthesis by forming a tripartite

complex with undecaprenyl-coupled intermediates and membrane lipids. *Nat. Commun.* **2020**, *11*, 1455.

(48) Efthimiadou, E. K.; Psomas, G.; Sanakis, Y.; Katsaros, N.; Karaliota, A. Metal complexes with the quinolone antibacterial agent N-propyl-norfloxacin: synthesis, structure and bioactivity. *J. Inorg. Biochem.* **2007**, *101*, 525–535.

(49) Huang, W.-Y.; Li, J.; Kong, S.-L.; Wang, Z.-C.; Zhu, H.-L. Cu(II) and Co(II) ternary complexes of quinolone antimicrobial drug enoxacin and levofloxacin: structure and biological evaluation. *RSC Adv.* **2014**, *4*, 35193–35204.

(50) Wang, X.; Du, Y.; Fan, L.; Liu, H.; Hu, Y. Chitosan-metal complexes as antimicrobial agent: Synthesis, characterization and Structure-activity study. *Polym. Bull.* **2005**, *55*, 105–113.

(51) Horvath, S. E.; Daum, G. Lipids of mitochondria. *Prog. Lipid Res.* **2013**, *52*, 590–614.

(52) Yarlagadda, V.; Sarkar, P.; Samaddar, S.; Haldar, J. A Vancomycin derivative with a pyrophosphate-binding group: a strategy to combat Vancomycin-resistant bacteria. *Angew. Chem., Int. Ed.* **2016**, *55*, 7836–7840.

(53) Le, J.; Liu, J.; Bo, Z.; Feng, X.; Kexue, Y.; Fujiang, W. The effect of Zn on the Zn accumulation and biosynthesis of amino acids in mycelia of *Cordyceps sinensis*. *Biol. Trace Elem. Res.* **2006**, *113*, 45–52.

(54) Lin, W.; Buccella, D.; Lippard, S. J. Visualization of peroxynitrite-induced changes of labile Zn²⁺ in the endoplasmic reticulum with benzo[*a*]pyrene-based fluorescent probes. *J. Am. Chem. Soc.* **2013**, *135*, 13512–13520.

(55) Eide, D. J. Zinc transporters and the cellular trafficking of zinc. *Biochim. Biophys. Acta* **2006**, *1763*, 711–722.

(56) Clear, K. J.; Harmatys, K. M.; Rice, D. R.; Wolter, W. R.; Suckow, M. A.; Wang, Y.; Rusckowski, M.; Smith, B. D. Phenoxide-bridged Zinc(II)-bis(dipicolylamine) probes for molecular imaging of cell death. *Bioconjugate Chem.* **2016**, *27*, 363–375.

(57) Rice, D. R.; Clear, K. J.; Smith, B. D. Imaging and therapeutic applications of Zinc(II)-dipicolylamine molecular probes for anionic biomembranes. *Chem. Commun.* **2016**, *52*, 8787–8801.

(58) DiVittorio, K. M.; Leevy, W. M.; O'Neil, E. J.; Johnson, J. R.; Vakulenko, S.; Morris, J. D.; Rosek, K. D.; Serazin, N.; Hilkert, S.; Hurley, S.; Marquez, M.; Smith, B. D. Zinc(II) coordination complexes as membrane-active fluorescent probes and antibiotics. *ChemBioChem* **2008**, *9*, 286–293.

(59) Kwong, J. M. K.; Hoang, C.; Dukes, R. T.; Yee, R. W.; Gray, B. D.; Pak, K. Y.; Caprioli, J. Bis(Zinc-dipicolylamine), Zn-DPA, a new marker for apoptosis. *Invest. Ophthalmol. Vis. Sci.* **2014**, *55*, 4913–4921.

(60) Chu, C.; Huang, X.; Chen, C. T.; Zhao, Y.; Luo, J. J.; Gray, B. D.; Pak, K. Y.; Dun, N. J. In vivo imaging of brain infarct with the novel fluorescent probe PSVue 794 in a rat middle cerebral artery occlusion-reperfusion model. *Mol. Imaging* **2013**, *12*, 8–16.

(61) Rathinakumar, R.; Walkenhorst, W. F.; Wimley, W. C. Broad-spectrum antimicrobial peptides by rational combinatorial design and high-throughput screening: the importance of interfacial activity. *J. Am. Chem. Soc.* **2009**, *131*, 7609–7617.

(62) Cabrini, G.; Verkman, A. S. Potential-sensitive response mechanism of diS-C3-(S) in biological membranes. *J. Membr. Biol.* **1986**, *92*, 171–182.

(63) Berney, M.; Hammes, F.; Bosshard, F.; Weilenmann, H. U.; Egli, T. Assessment and interpretation of bacterial viability by using the LIVE/DEAD BacLight Kit in combination with flow cytometry. *Appl. Environ. Microbiol.* **2007**, *73*, 3283–3290.

(64) Burow, L. C.; Mabbett, A. N.; Borrás, L.; Blackall, L. L. Induction of membrane permeability in *Escherichia coli* mediated by lysis protein of the Cole7 operon. *FEMS Microbiol. Lett.* **2009**, *298*, 85–92.

(65) Swain, J.; El Khoury, M.; Flament, A.; Dezanet, C.; Brie, F.; Van Der Smissen, P.; Decout, J. L.; Mingeot-Leclercq, M. P. Antimicrobial activity of amphiphilic neamine derivatives: understanding the mechanism of action on Gram-positive bacteria. *Biochim. Biophys. Acta, Biomembr.* **2019**, *1861*, 182998.

(66) Wood, S. J.; Miller, K. A.; David, S. A. Anti-endotoxin agents. 1. Development of a fluorescent probe displacement method optimized for the rapid identification of lipopolysaccharide-binding agents. *Comb. Chem. High Throughput Screening* **2004**, *7*, 239–249.

(67) Ling, L. L.; Schneider, T.; Peoples, A. J.; Spoering, A. L.; Engels, I.; Conlon, B. P.; Mueller, A.; Schäberle, T. F.; Hughes, D. E.; Epstein, S.; Jones, M.; Lazarides, L.; Steadman, V. A.; Cohen, D. R.; Felix, C. R.; Fetterman, K. A.; Millett, W. P.; Nitti, A. G.; Zullo, A. M.; Chen, C.; Lewis, K. A new antibiotic kills pathogens without detectable resistance. *Nature* **2015**, *517*, 455–459.

(68) Lee, W.; Hwang, J. S.; Lee, D. G. A novel antimicrobial peptide, scolopendin, from *Scolopendra subspinipes mutilans* and its microbicidal mechanism. *Biochimie* **2015**, *118*, 176–184.

(69) Dewan, P. C.; Anantharaman, A.; Chauhan, V. S.; Sahal, D. Antimicrobial action of prototypic amphipathic cationic decapeptides and their branched dimers. *Biochemistry* **2009**, *48*, 5642–5657.

(70) Zorko, M.; Jerala, R. Alexidine and chlorhexidine bind to lipopolysaccharide and lipoteichoic acid and prevent cell activation by antibiotics. *J. Antimicrob. Chemother.* **2008**, *62*, 730–737.